AN ABSTRACT OF THE DISSERTATION OF

Jintana Nammoonnoy for the degree of Doctor of Philosophy in Chemistry presented on September 7, 2010
Title: A Photoactivable Microfluidic Device for Heavy Metal Ion Extraction

Abstract approved:

_____

Vincent T. Remcho

The development of microfluidic devices for heavy metal extraction is presented in this dissertation. Various research areas, covering subjects from photochromic compound syntheses to microchip fabrication techniques are explored to develop microfluidic devices capable of extracting heavy metal ions from drinking water. Through integration of the beneficial characteristics of both microfluidic devices and photochromic dyes, a simple and innovative microchip configured as a photoactivable extraction system for metal ion accumulation and release can be realized.

The initial research focused on the utilization of photochromic compounds namely spiropyrans, as chelators for heavy metal extraction. Spiropyrans are organic photochromic compounds that have been widely studied. Upon irradiation with UV or visible light, spiropyrans isomerize between the closed and open forms, in which the open form is comparatively more polar. Metal ions can influence this isomerization process by associating with the open form through the electron-rich oxygen atom. In

contrast, visible light produces a high concentration of the closed form, and thus hinders metal-binding. Spiropyrans, therefore, show great potential as photo-reversible metal-complexation agents. The spiropyran derivatives were synthesized and immobilized on solid supports including polymeric resins and poly(methylmethacrylate) (PMMA) microchips. Metal ion uptake can be triggered using UV light and subsequently reversed on demand by shining green light on the colored complex, which regenerates the inactive spiropyran form resulting in the release of metal ions. The use of light to trigger the chelator offers unique opportunities.

The work continued with the development of microfluidic fabrication for creating versatile, solvent-compatible microfluidic devices through surface modification. There are challenges associated with the use of polymeric based microfluidic devices, particularly in surface modification steps, as solvents can embrittle thermoplastics that resulting in microcracking. To overcome this limitation, we explored the possibility of fabricating extremely robust microfluidic devices entirely from fluorocarbon and glass materials. The work demonstrated a new fabrication technique based on a chemically activated poly(tetrafluoro ethylene) (PTFE) sheet sandwiched between chemically activated glass substrates. The PTFE microchannels can be fabricated in minutes using a cutting plotter to create microchannels. The possibility of glass to PTFE makes this method applicable in a wide range of applications.

A Photoactivable Microfluidic Device for Heavy Metal Ion Extraction

by
Jintana Nammoonnoy

A DISSERTATION

submitted to

Oregon State University

in partial fulfillment of
the requirements for the
degree of

Doctor of Philosophy

Presented September 7, 2010
Commencement June 2011

Doctor of Philosophy dissertation of Jintana Nammoonnoy presented on September 7, 2010

APPROVED:

_____

Major Professor, representing Chemistry

_____

Chair of the Department of Chemistry

_____

Dean of the Graduate School

I understand that my dissertation will become part of the permanent collection of Oregon State University libraries. My signature below authorizes release of my dissertation to any reader upon request.

_____

Jintana Nammoonnoy, Author

ACKNOWLEDGEMENTS

I would like to thank my many friends, especially Saowalee Jongrattananon, Pimonpan Sakornchareon, Panumart Chaikham, Lalita Attanatho, and Hasini Perera for the moral support and encouragements throughout these years.

I also would like to acknowledge the Royal Thai Government for financial support and thank all the staffs at the Royal Thai Embassy in Washington DC for taking care of me during my stay in at OSU.

I thank the Department of Chemistry at OSU, the faculty, staff and all the facilities that were available to me to complete my work.

And most importantly, I would like to thank my family, especially my mother and my father; for their endless love and supports during my stay here to continue my education study at OSU.

CONTRIBUTION OF AUTHORS

My research advisor, Dr. Vincent T. Remcho, edited and assisted in writing all chapters of this dissertation. His name appears on all published and submitted work contained herein. My co-advisor Dr. Jeffrey R. Walker, edited and assisted in writing all chapters of this dissertation. Taehyeong Kim collaborated and contributed in designing of Chapter 4 of this dissertation.

TABLE OF CONTENTS

TABLE OF CONTENTS (Continued)

TABLE OF CONTENTS (Continued)

LIST OF FIGURES

LIST OF TABLES

CHAPTER 1

INTRODUCTION TO PHOTOCHROMISM AND TO MICROFLUIDIC DEVICES

This chapter is divided into two sections. The first section provides an introduction to the synthesis and properties of photochromic compounds. The next section highlights advances and challenges in the fields of microfluidics and fabrication technologies. These discussions are intended to provide background and familiarity with recent developments in the areas of photochromic compounds and microfabrication techniques. Microfluidic chips have been fabricated with the aim of utilizing spiropyran chemistry in a format that maximizes surface area/volume ratio. The applications of photochromic compounds for heavy metal extraction using microfluidic devices as a platform and novel microfabrication techniques will be discussed in chapters 2, 3, and 4.

1.1. Photochromism

The ability to reversibly manipulate the physical and chemical properties of a material with an external stimulus forms the basis of stimuli-responsive systems. The use of light as a trigger is particularly attractive since its characteristics can be remotely and accurately controlled, quickly switched and easily focused into specific areas. New tailorable materials have emerged in areas including nanotechnology, electronics, diagnostics and therapeutic biomedicine with properties, such as

conformation shape, phase, wettability, permeability, and solubility, able to be reversibly transformed with light stimulation.

Photochromism can be defined as a reversible transformation of chemical species, induced in one or both directions by electromagnetic radiation, between two stages having observable light absorptions in different regions.

$$A(\lambda_1) \quad \underset{h\upsilon_2,\, \Delta}{\overset{h\upsilon_1}{\rightleftharpoons}} \quad B(\lambda_2)$$
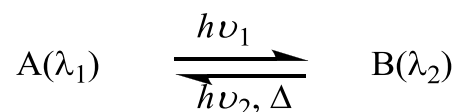
Photochromism involves the reversible transformation of chemical species between two isomeric forms induced by the absorption of light which results in a change in absorption spectra. Ordinarily, the photochromic reaction involves a reversible transformation between two species with **B** having at least one absorption band appearing at longer wavelength than those of **A**. The activating radiation generally is in the UV region (300-400 nm) and the reverse reaction (B→A) can be in the visible (400-700 nm). The photoconversion mechanism includes pericyclic reactions, *cis-trans* isomerizations, dissociation processes, intramolecular hydrogen transfers or group transfers, and electron transfers (oxidation-reduction). In addition to a color change, these transformations are accompanied by changes in the physical and chemical properties of the species involved, such as alterations in the dipole moment, refractive index or geometric structure. Importantly, these dynamic transformations can generate coincident changes in the optical, chemical, electrical and bulk properties of the system that incorporates them. Photochromic molecules therefore play an

important role within photo-responsive systems, being able to capture an optical signal and then convert it via isomerization, to useful property change.

Photo-responsive systems involve transformations which are notably unimolecular processes and reversible. The transformations depicted in Figure 1.1 can be described briefly as follows:

1. Ultraviolet (UV) irradiation of an azobenzene stimulates the conversion of the planar *trans* isomer to the bent *cis* isomeric form via the isomerization of a –N=N- bond.

2. UV irradiation of spiropyrans and spirooxazines initiates an electrocyclic ring opening reaction of a spiro form which results in the formation of an open, planar merocyanine form with an extended conjugated system able to absorb strongly in the visible region.

3. For diarylethenes UV irradiation results in the closing of the six-membered ring within its core which results in the formation of thermally irreversible colored isomers [1].

The photochromic inter-conversion between isomeric forms often referred to as switching.

a)

Azobenzenes

UV →
← Δ or visible

trans form

cis form

b)

Spiropyrans

UV →
← Δ or visible

closed form
(SP)

open form (Merocyanine)
(MC)

c)

Spirooxazines

UV →
← Δ or visible

closed form
(spiro)

open form (Merocyanine)
(Quinoic form)

d)

Diarylethenes

UV →
← Δ or visible

open form

closed form
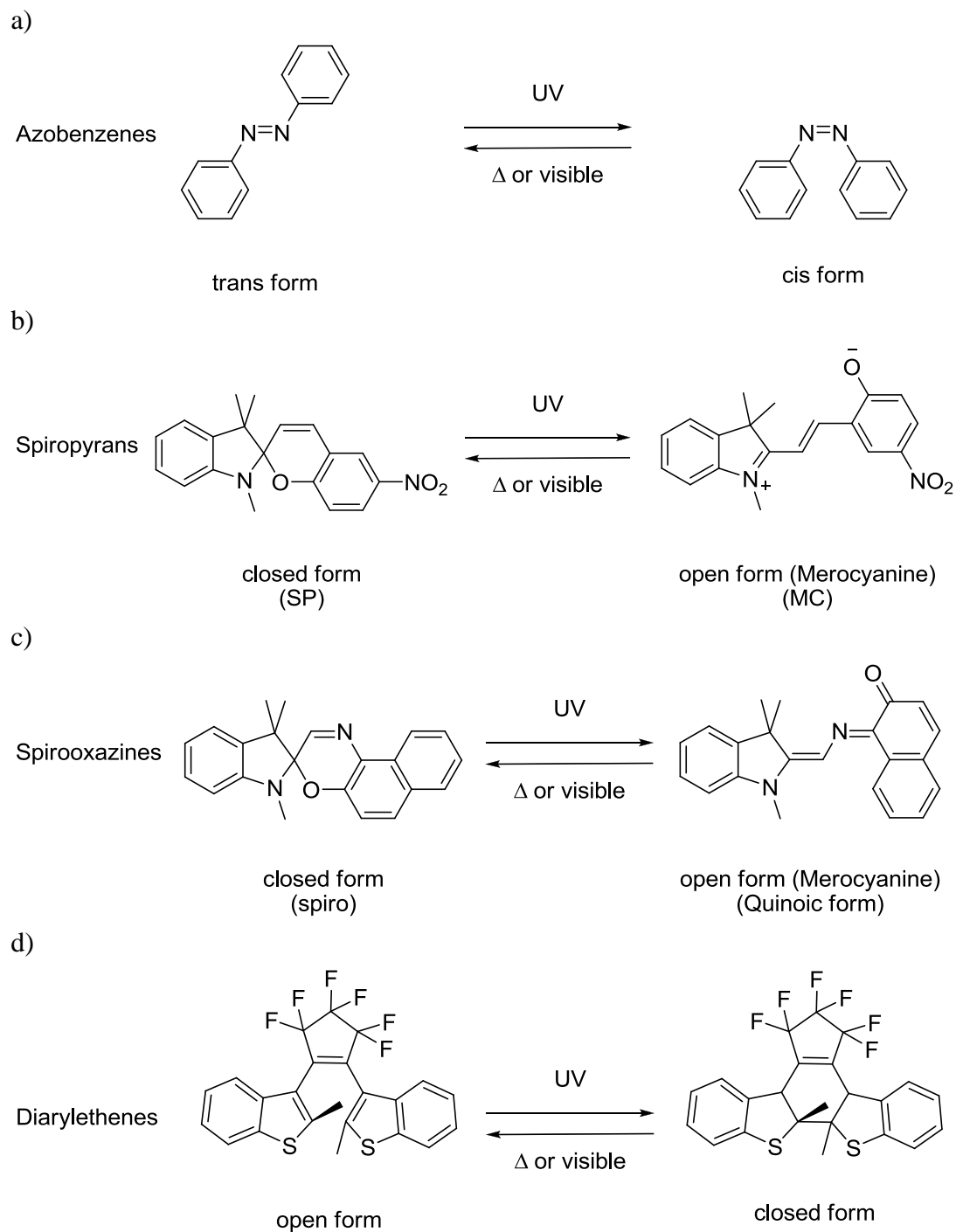
Figure 1.1 Families of photochromic compounds commonly used in polymeric systems [2].

1.1.2. Spiropyrans

Spiropyrans are members of a class of photochromic compounds that have continued to attract the attention of scientists for over 20 years [3-18]. The photochromism of spiropyran was discovered independently by Fischer and Hirshberg, and by Chaude and Rumpf [19, 20]. Due to their remarkable ability to reversibly change between two forms with different absorption spectra under the action of electromagnetic radiation, they find application in non-linear optics, modern optical information carriers, molecular-scale logic switches, and other nanodevices [21-26]. Spiropyrans are photochromic organic compounds composed of two heterocyclic parts linked together by a tetrahedral sp^3 spiro carbon atom. Irradiation of a spiropyran with UV light induces heterolytic cleavage of the spiro carbon-oxygen bond, producing the open form of the ring, the intensely colored merocyanine (Figure 1.1b). The merocyanine (MC) reverts to the initial spiropyran (SP) form in the dark or by visible light irradiation. The time required to resume the closed form depends on the temperature and on the nature of the compound [27]. Merocyanines present a characteristic absorption band in the visible spectral region between 570 and 610 nm depending on the polarity of the solvent. The equilibrium between SP and MC is depicted in Figure 1.1b.

The transition between forms SP and MC of these compounds proceeds reversibly by both photochemical and thermal mechanisms, and also under the action of chemical reagents (protons, metal ions) [28, 29]. Thus, their chemical structure and spectral properties can be controlled using external controls, e.g., illumination with a

definite wavelength. An important challenge in the chemistry of spiropyrans is their photostability. The simplest way to achieve this is by employing spirooxazines, which are resistant to photodegradation [30].

Spiropyrans were convenient subjects for studying the photophysical properties of merocyanines including photoisomerization and excited-state relaxation [31]. By their example, it was shown that substituent groups of merocyanines have a substantial effect on their photophysical properties, particularly, the photoisomerization process [28, 31]. For example, the introduction of a nitro group into the benzene ring of a spiropyran substantially increased the yield of the triplet state, the formation of which often precedes the *cis-trans* isomerization (i.e., the transition between the closed and open forms) [29, 32-34]. Raman spectroscopic studies of the aggregations formed by open spiropyrans have shown that the $6-NO_2$ group stabilizes this structure due to its electrostatic interaction with the positively charged nitrogen atom of the heterocyclic moiety of the neighboring molecules [30].

1.1.3. Spiropyran Synthesis

A spiropyran can be synthesized via several different routes. As indicated in Figure 1.2, one can connect the two "halves" of the molecule by condensing an intermediate providing the C^2 and C^3 atoms of the pyran ring. Another half provides the C^4, C^5, C^6 and the oxygen atoms of the pyran ring. In a second approach, one intermediate is the source of C^2, C^3, and C^4, while the other provides C^5, C^6, and

oxygen atom. In the third approach, one can prepare a spiropyran and then introduce new substituents, or transform substituents already present.

Figure 1.2 Spiropyran synthesis [1].

The first method is the most common, and is exemplified by the condensation shown in Figure 1.3 of a 2-alkyl heterocyclic quaternary salt or the corresponding methylene base with 2-hydroxy aldehyde group. These intermediates have given a broad assortment of spiropyran classes. The readily available 1,2,3,3,-tetraalkyl-3*H*-indoleninium salts and salicylaldehydes has led to a large number of spiro-(2*H*-1-benzopyran-2,2´-indolines). A common acronym for this class, "BIPS" will be used in this chapter as both singular and plural.
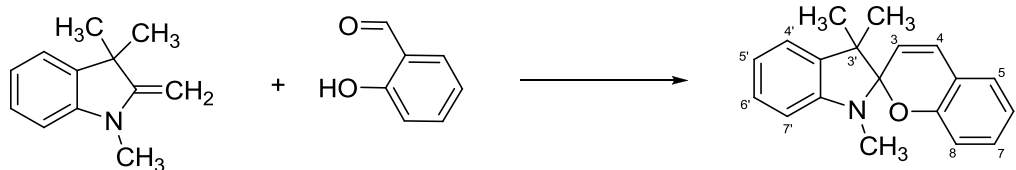
Figure 1.3 The condensation of salicylaldehyde and 1,2,3,3-tetramethyl-3H-indoleninium salt gives rise spiropyran derivative [1].

The second method corresponds to moving the formyl group from the aldehyde intermediate to the methylene base, and is a standard method for preparing a

merocyanine. The method is useful for the reaction of easily obtained and stable Fischer's aldehyde (2-formylmethyleneindolines) with ketomethylene compounds such as 2-hydroxybenzofuran or 2-hydroxybenzothiophene where the corresponding hydroxyaldehyde is difficult to obtain (Scheme 1.4). These two methods include the several routes that can lead to various symmetrical and unsymmetrical spiro(dipyran) [35].
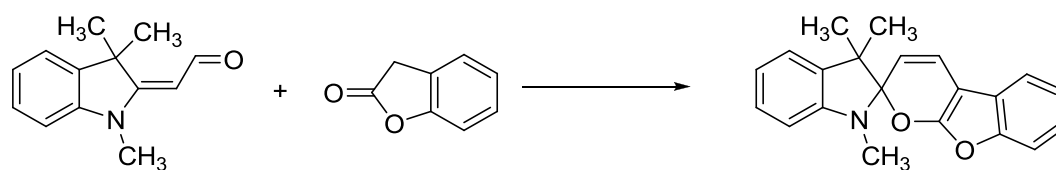
Figure 1.4 The synthesis of spiropyran using 2-formylmethyleneindoline and 2-hydroxybenzofuran [1].

The third approach is useful when spiropyran itself is easily available, the necessary substituted intermediates are not, and the spiropyran tolerates the chemical transformations involved. Halogenation and nitration of BIPS and spiro(dinaphthopyrans) can be carried out by standard methods bromo substituents replaced by cyano or lithium, nitro substituent groups reduced to amino, etc. For example, Tanaka et al. synthesized spiropyran derivatives carrying an oxymethylcrown ether moiety by converted the chloromethyl group in 8-chloromethyl spiropyran to oxymethylcrown ether (Figure 1.5) [36].
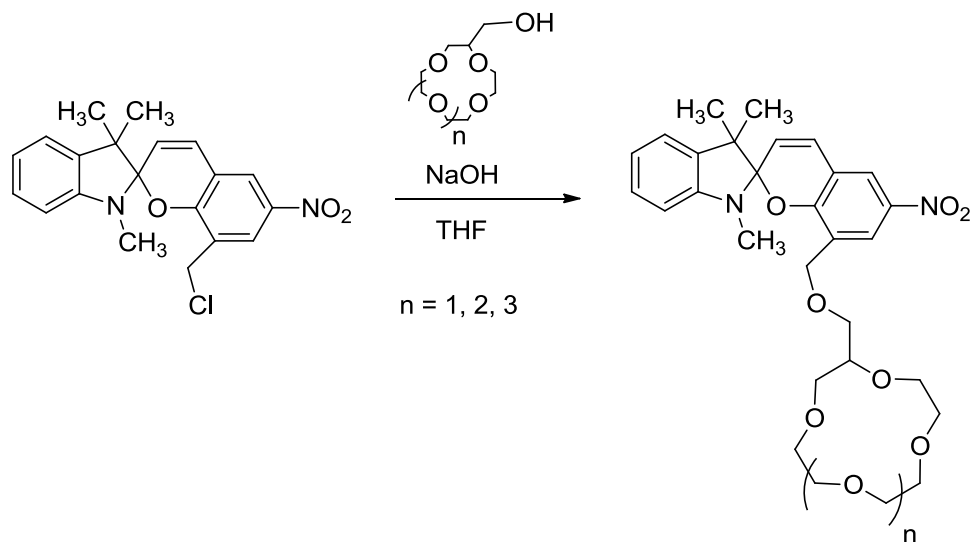
Figure 1.5 The synthesis of oxymethylcrowned spiropyran [36].

1.1.4. Applications and future trends

The chemical transformation between spiropyran (SP) and merocyanine (MC) has attracted great attention because the molecular properties change enormously through a very basic unimolecular reaction. The large change in the molecular properties has led to great interest in using these molecules as component for sensors and detectors [37], in light-sensitive eyewear [38], to perform logic operations in molecule-based devices [11, 39] and to induce reversible changes in chemical or optical properties of organic-inorganic interfaces [40].

Practical application of photochromism at first (ca 1955-1970) concentrated on the spiropyrans, and especially on BIPS compounds, because of their availability, photosensitivity, convenient thermal fade rates, and good color contrast when perceived by the human eye. Photochromic plastic ophthalmic sunglasses are the

largest volume and value application for photochromics, but the spiropyrans originally used generally underwent photodegradation rapidly in sunlight, a serious deficiency for this application. The emphasis then shifted to spironaphthoxazines which generally were more resistant to photodegradation [41]. The first commercial plastic photochromic lens was the Photolitem lens, introduced by American Optical in 1982. The matrix for the lens was the polymer from allyl diglycol carbonate, the most common matrix for plastic ophthalmic lenses. The Photolite lens contained an indoline spironaphthoxazine as its photochromic component. The photochromic reaction of the spironaphthoxazines is well known (Figure 1.6) [38]. However, applications in which the dye was required to undergo numerous cycles or be irradiated continuously were impractical because of the rapid fatigue of these dyes [42].
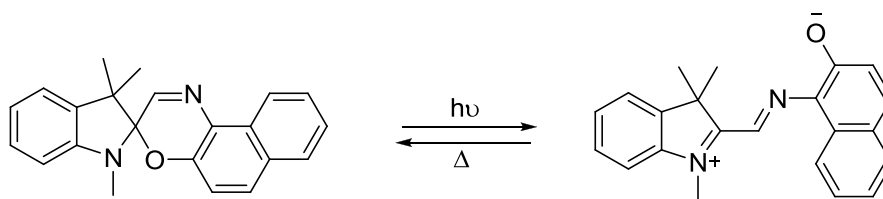
Figure 1.6 The photoconversion of spironaphthoxazine [38].

The spectral properties of merocyanines (particularly fluorescence) strongly depend on environmental characteristics, namely, solution polarity and viscosity. Due to these properties, merocyanines were among the first reference points used in building the scales of solvent polarity, for determination of water content in organic solvents and have also found application as sensors, probes and markers in chemical analysis [16, 24, 37, 43-47].

The photoinduced inter-conversion of the two states of a photochromic compound can be exploited to modulate the emission of a fluorescent partner. This photo-response can be facilitated through the FÖrster resonance energy transfer (FRET) process where both fluorescent and photochromic components are normally integrated within the same macromolecular or nanostructured construct. The mechanism initially requires two fluorescent dyes: the fluorescent donor emits high-energy photons and the fluorescent acceptor emits low-energy photons. When the donor and acceptor approach each other near or within the FÖrster distance, fluorescence color switches from donor to the acceptor, or from high-to-low-energy photons. Li et al. used such spiropyrans to fabricate nanoparticles, whose fluorescence color can be optically switched from one color to another (Figure 1.7). The resulting nanoparticle fluorescence is at least 30 times brighter than conventional organic dyes. Tuning the copolymer composition and sequences effectively reduces nonspecific interactions between nanoparticles and cell membranes. Such feature-packed nanoparticles advanced further biomedical imaging capabilities such as cell construction, spectroscopic characterization and initial live cell imaging results [48].

spiro-form   mero-form
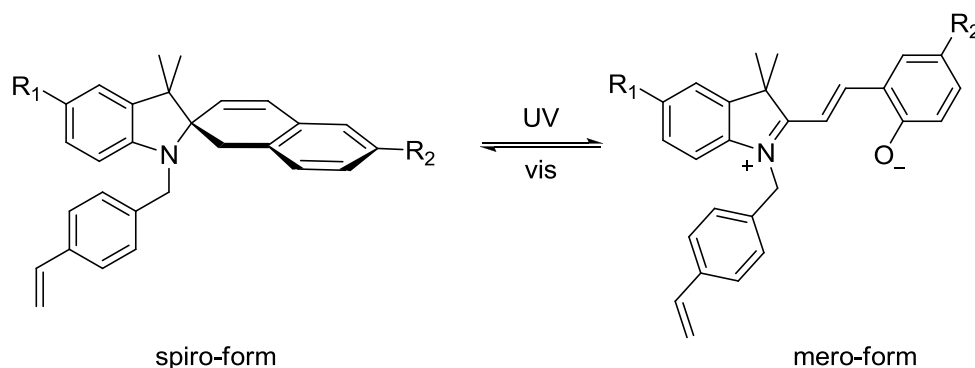
SP: R$_1$= H, R$_2$=NO$_2$,

MSP: R$_1$= OMe, R$_2$=NO$_2$,

MCSP: R$_1$= OMe, R$_2$=CN, CSP: R$_1$= H, R$_2$=CN

Figure 1.7 Chemical structures illustrate the spiro and mero forms of the photoswitchable fluorescent dyes and how photochemical reactions switch red fluorescence to dark state (SP), green fluorescence (MSP), and blue fluorescence (MCSP and CSP) [48].

One of the most widely studied applications of spiropyrans capitalizes on their intense absorption in the visible region which is of great utility in assembling molecular switching systems, where the photochromic compound can be used to represent two digital codes "0" or "1" as different absorption spectra. Kanashi et al. have shown the potential application of two kinds of bi-functional photochromic compounds combinations of spiropyran and azobenzene derivatives, as four digit codes for multi-addressable systems and molecular switching [49].

The pronounced negative metallochromism of the merocyanine form of spiropyrans was associated with the possibility for a metal cation to coordinate the oxygen atom of oxyphenyl residue that carries a considerable negative charge. This

effect was enhanced by the introduction of metal ions into coordination spheres, most often these were crown and azacrown groups (Figure 1.8) [50-52]. Furthermore, numerous spiropyran derivatives have been designed and utilized for optical sensing for neutral molecules, such as nucleobases [53], amino acids and DNA [54, 55].
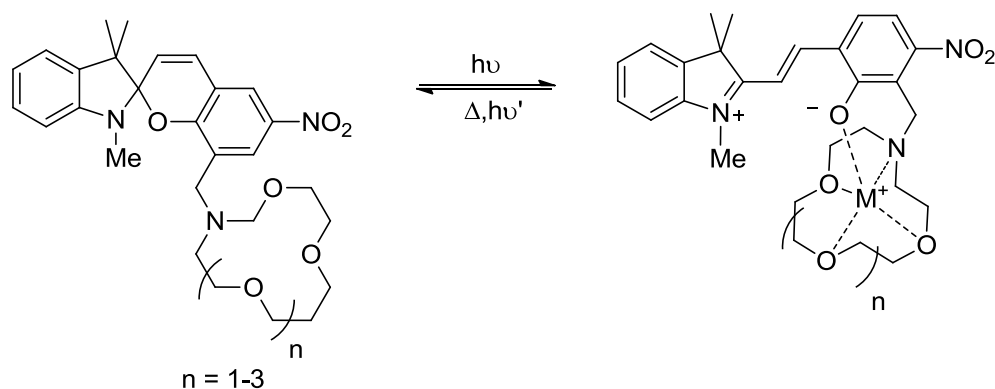
Figure 1.8 Photoconversion of crowned spiropyran.

1.2. Microfluidic devices

1.2.1. Introduction to microfluidics

"Microfluidics" is the field of miniaturization that deals with the behavior, precise control and manipulation of fluids that are geometrically constrained to a small scale, typically sub-millimeter. Microfluidic channels can be less than 100 μm wide. This allows them to handle biological materials such as DNA, proteins or cells in minute quantities-usually nano-liters or pico-liters. The advantages of these approaches include reduced sample and reagent consumption, reaction time, analysis time, experimental footprint and increased assay parallelization, automation and portability. Microfluidics not only enable very precise analysis, they also open up the

potential for the manipulation of living matter by mixing, separating and handling different components on the nanoscale. Microfluidic devices have allowed for the development of portable instrumentation requiring only small power supplies.

Although microfluidic devices may be produced from glass, quartz, silicon, and various polymeric materials, glass substrates have been employed most frequently owing to their favorable optical properties, chemical resistivity, and support of reproducible electroosmotic flow [56-60]. Fabrication of glass microfluidic devices usually involves micro channel/structure fabrication using photolithographic and wet-etching procedures, followed by bonding the etched plate to a flat cover plate.

The bonding of glass substrates is one of the most important and time-consuming steps in the fabrication of glass microchips, and to realize their mass production, an improvement in the bonding process is critically important to achieve high throughput and yield. A variety of bonding techniques has been reported including field-assisted bonding (anodic bonding), thermal bonding, low-temperature bonding, bonding with hydrofluoric acid (HF bonding), and bonding with sodium silicate or adhesives as intermediate layers. In order to obtain a strong bond via a chemical reaction between hydroxyl-groups on glass surfaces, direct bonding is prefered at high annealing temperature (typically between 500-650 °C) for glass-glass fusion [57, 58, 61, 62]. Anodic bonding (or field-assisted bonding) is done at moderate temperatures (150–500 °C), and utilizes a large electric potential (200–1500 V) to create a robust, leak-free silicon–glass bond [63]. Due to the large attractive forces

generated by the electric field, anodic bonding has less stringent requirements for the surface quality of substrates and particle contamination compared with fusion and direct bonding. Direct bonding can also be performed below fusion temperature. Low-to-intermediate temperature bonding usually involves the use of various adhesives below 100 °C [61, 64, 65]. Such procedures are suitable for the fabrication of microfluidic devices containing structural features that do not require resistance to high temperatures, such as electrodes and waveguides; however, low-to-intermediate temperature direct bonds are not as robust as fusion bonds. In adhesive bonding, an intermediate adhesive layer is conveniently used to create a bond between two surfaces to hold them together.

Initially, microfluidic devices were predominantly fabricated using glass or silicon substrates. The fabrication of glass microchips is often expensive, time consuming, and the process involves the use of harmful hydrofluoric acid (HF) and clean room facilities. These disadvantages have encouraged manufacturers to seek alternative materials for microchips fabrication. Polymer materials and their fabrication methods proved to be the solution to these challenges. Polymer substrates also offer excellent optical characteristics, temperature stability, chemical resistance and biocompatibility. Together with the ease of fabrication and greater flexibility over silicon and glass, these characteristics make polymer substrates highly adaptable for microfluidic applications. Compared with traditional microfluidic materials such as silicon or glass, polymers offer substantially lower raw material and manufacturing costs.

Thermoplastics are a class of synthetic polymers that exhibit softening behavior above a characteristic glass transition temperature (T_g) resulting from long-range motion of the polymer backbone, while returning to their original chemical state upon cooling. Thermoplastic polymers differ from elastomer or thermoset plastics by their ability to be softened or fully melted and reshaped upon heating, while remaining chemically and dimensionally stable over a wide range of operational temperatures and pressures. The various thermoplastic polymers including polymethylmethacrylate (PMMA), polycarbonate (PC), and cyclic olefin-polymers (COP) or -copolymer (COC) have been widely used as materials in microfluidics.

Elastomeric polymers, especially polydimethylsiloxane (PDMS), have also gained much popularity as materials for microfluidics fabrication. PDMS has a number of useful properties including its chemical resistance, optical transparency (down to ~300 nm), thermal stability (below 150°C), physical toughness and flexibility [66-68]. Due to the wide range of polymers available, they are highly attractive as substrates for microfluidic systems as revealed by a search of the Thomson Reuters ISI and National Institutes of Health PubMed databases. As shown in Figure 1.9, silicon and silica remain the dominant materials for microfluidics, and with expanding research attention, thermoplastics have demonstrated a great growth trend in the microfluidics industry.
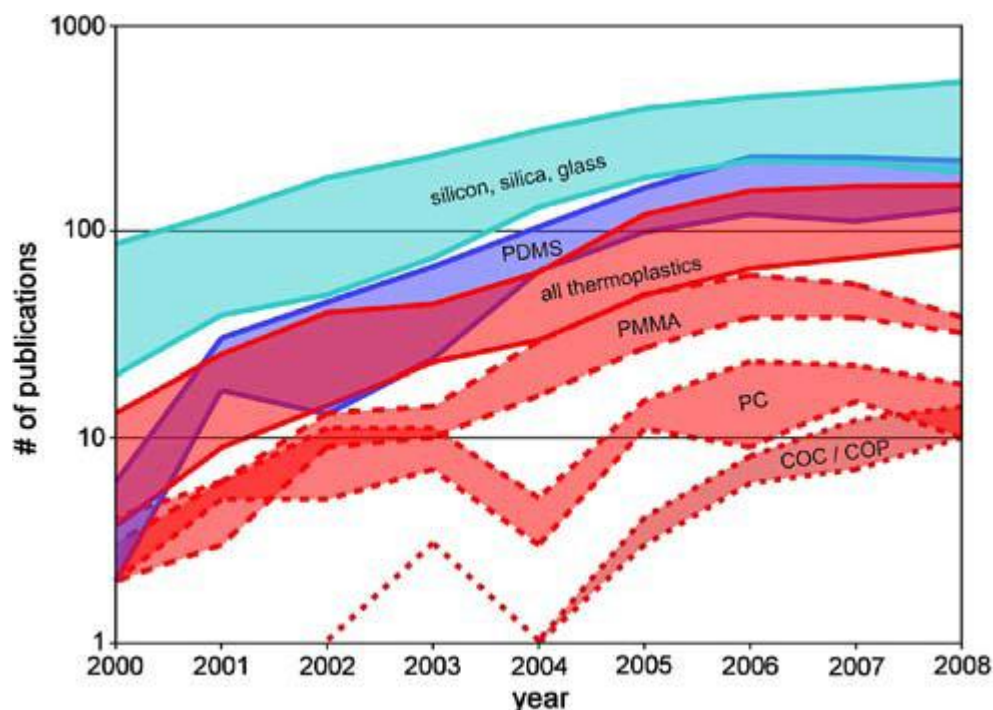
Figure 1.9 Approximate numbers of annual publications referencing different materials for microfluidics. Maximum and minimum values defining the ranges were extracted from the Thomson Reuters ISI and NIH PubMed databases, respectively. Data for 2008 is projected based on reference counts from the first half of the year [69].

1.2.2. Methods of fabrication

Microchannel fabrication has been reported using a variety of replication methods including hot and cold embossing, injection molding, and thermoforming [70-73]. In addition, thermoplastics can also be directly machined using laser ablation, mechanical micromilling, and solvent etching techniques [74-76]. Figure 1.10 gives a schematic overview of polymer fabrication process steps for microfluidic systems. Usually, the fabrication procedure for microfluidic devices consists of three main steps; master fabrication, replication of channel plates, and bonding.
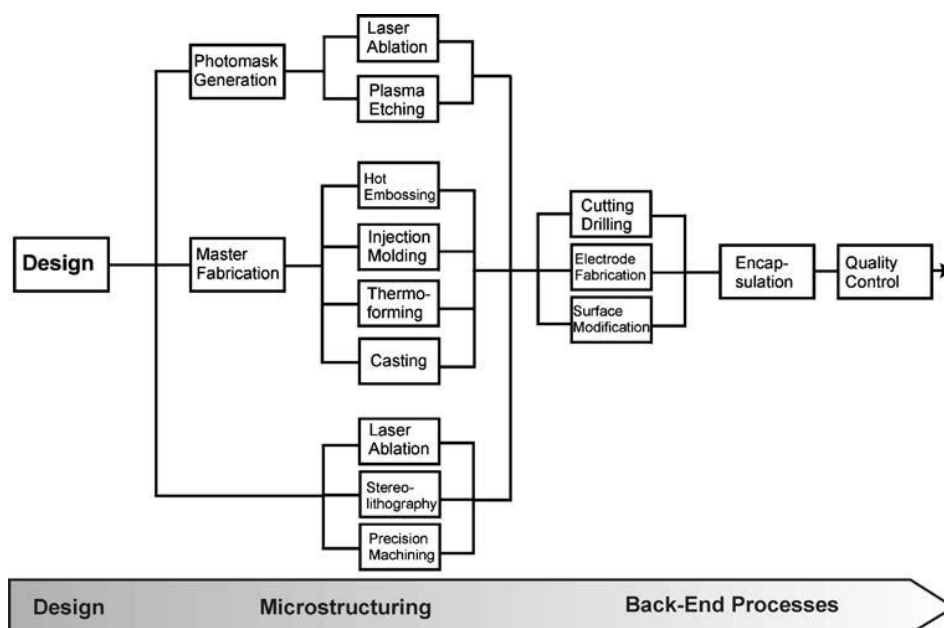
Figure 1.10 Process diagram of polymer microfabrication technologies [77].

1.2.2.1. Fabrication of channel plate

As indicated previously, polymeric microfluidic chips are usually composed of channel plates and cover plates (or cover films) that must be bonded to form complete microfluidic chips. Channel plates have been fabricated using a wide variety of fabrication techniques such as hot and cold embossing, injection molding, laser ablation, *in situ* polymerization, and solvent etching.

1.2.2.1.1. Hot embossing

Hot embossing is the most commonly used method for the replication of polymeric microchannels. There, a polymer plate is placed on the surface of a master bearing raised microscale features. The assembly is mounted in a press and embossed under a controlled pressure. The system is then heated to a temperature just above the

T_g of the polymer material. The channel plate is demolded from the master template when the temperature cools down below the T_g. To obtain a quick overview, Table 1.1 summarizes the compilation of physical and chemical properties of the most widely used polymers for microfluidic applications.

Table 1.1 Overview of polymer material properties [78].

Name	Density (g·cm^{-3})	T_g (°C)	Heat distortion temperature (°C)	Resistivity (Ω cm^{-1})	Water absorption (%)	Refractive index	Young's (tensile) modulus (MPa)	Thermal expansion coeff. (10^{-6}/K)	Resistant against	Not resistant against
PMMA	1.19	110	90	1×10^{15}	2	1.492	3200	80	Acids, bases (medium conc.), oil petrol	Alcohols, acetone, benzole, UV light
PC	1.19-1.24	148	125	1×10^{14}	0.30	1.58-1.6	2200-2400	70	Alcohols, acids	Hydrocarbons, ketones, KOH
PP	0.9	0-10	100-110	$>1\times10^{14}$	0.01-0.1	1.49	1450	100-200	Acids, bases, alcohols, organic solvents, fats	Petrol, benzole, hydrocarbons
PS	0.9-1.24	100	70	$>1\times10^{16}$	<0.4	1.59	2300-4100	30-210	Bases, alcohols	Conc. Acids, ether, hydrocarbons
PE (LD/HD)	0.91 (LD) 0.967 (HD)	110/1140	80/100	10^{15}-10^{18}	<0.015	1.51 (LD)	200/1000	170/200	Acids, bases, alcohols, oil	hydrocarbons
COC	1.02	78	170	$>1\times10^{14}$	0.01	1.53	2600	70	Acids, bases	
COP	1.01	138	140	$>1\times10^{17}$	0.01	1.525	2400	70		
PEEK	1.3	143	250	$>1\times10^{16}$	0.5		3700	17	Most organic and inorganic substances	Conc. Nitric acid, sulfuric acid, UV light
PDMS	1.03	-120	200	1.2×10^{14}	0.1	1.43		960	Weak acids and bases	Strong acids, hydrocarbons
SU-8	1.19	210	-	2.8×10^{16}		1.58	2000	52	Acids, bases, most solvents	
PI	1.42	360-410	400	$>1\times10^{12}$	2.9-4	1.7	2500	20	Acids, bases, solvents	

1.2.2.1.2. Cold embossing

Xu et al. have demonstrated the imprinting of polymeric microfluidic channels from silicon templates at room temperature under the application of high pressure (2700 psi) [71]. The plastic plate is placed on a silicon template and the whole assembly is sandwiched between two polished aluminum plates. A hydraulic press is employed to apply high pressure at room temperature. When the pressure is released, the open channels on the plastic substrate are sealed with a layer of a layer of PDMS film to form a complete microchannel. This approach avoids the necessity of heating the plastic substrate during the stamping process. Since no external heating is involved, one template can be used to imprint scores of microfluidic devices.

1.2.2.1.3. Injection molding

The raw material employed for the injection molding is supplied in granular form. Polymer pellets are melted in a heated cylinder. The molten polymer material is injected under high pressure into a mold cavity containing an inserted master. The template masters are usually made from nickel or silicon and are employed to define the geometry of the microfluidic parts. Finally, the cavity is cooled for demolding. Injection molding is a promising approach for the mass production of plastic microfluidic chips and is an industry mainstay.

1.2.2.1.4. Laser ablation

Laser ablation has been widely employed to fabricate polymer microchips [74, 78]. The microfluidic structures are designed using common drawing tools such as

Solidworks (Dassault Systèmes SolidWorks Corp., MA, USA) or AutoCAD (Autodesk, Inc., CA, USA). The pattern is then sent to the laser scriber for automatic machining on the polymer substrate. In the process, a high energy laser beam is used to break bonds in polymer molecules and to remove the decomposed fragments from the ablation regions. Usually, a commercially available laser scriber is used to engrave the plastic substrate. This consists of an eximer laser and an XY table on which the plastic plate is mounted. A focused laser beam scanned over a 2-D area by the combined motion of the X and Y stages. The substrate is fixed on a platform that can move in the Z-axis.

1.2.2.1.5. Solvent etching

In 2005, Brister *et al*. introduced a very simple method for microfluidic fabrication by solvent etching. Patterned PDMS is used as a template to control the flow path of an etching solvent through a channel design to be replicated on the plastic substrate. The etching solvent is a mixture of organic solvent depending on the material of the substrate. This approach provides an alternative way for rapid microfluidic fabrication.

1.2.2.2. Bonding

Regardless of the fabrication method employed, the sealing of the open microchannels is necessary to produce the final enclosed fluidic paths without clogging the channels, changing their physical parameters, or altering their dimensions. This often presents a unique set challenges in microchip fabrication.

There are a number of considerations that must be taken into account when selecting and implementing an appropriate bonding method. Bond strength is a critical consideration, with some applications requiring interfacial bond energies on par with the cohesive strength of the bulk substrate material, and others benefiting from relatively weak and reversible bonds. Bond interfaces must provide suitable chemical or solvent compatibility to prevent degradation during use, without compromising dimensional control of the microchannels due to deformation during the bonding process. Other important considerations for the bond interface include surface chemistry, optical properties, and material compatibility and homogeneity of the channel sidewalls.

1.2.2.2.1. Thermal bonding

A Variety of thermal bonding techniques have been widely used to allow the formation of microchannels from dissimilar materials. Usually, the channel plate and the cover plate are assembled with the microstructures enclosed inside and are heated to a temperature above the T_g of the polymer material in a convection oven while pressure is applied on the assembly in a press [79]. However, slight variances in pressure and temperature may lead to deformation of the channels and adversely affect reproducibility. To overcome these limitations, hot-press bonding has been demonstrated in a vacuum or in a hot water bath for sealing PMMA microchips [80, 81].

1.2.2.2.2. Solvent bonding

When a plastic surface is solvated, polymer chains become mobile and can readily diffuse across the solvated layer, leading to extensive intertwining of chains between the surfaces resulting in exceptionally strong bonds [69, 82-85]. Solvent may be applied to the polymer substrates in either liquid or vapor phase. Since the bonding process is conducted at room temperature, thermal distortion of the microstructures can be avoided. Depending upon the specific approach used, solvent bonding can be a high throughput process that is readily scalable from prototyping to mass production. However, there are some disadvantages as the solvents can cause clogging or channel deformation during sealing. In order to prevent excessive solvent uptake into the polymer matrix which can lead to channel deformation during bonding, usually a sacrificial layer is used to protect the channel during bonding [86]. Prior to sealing, the channel is filled with paraffin wax that forms a solid sacrificial layer at room temperature [87]. Once the sealing step was complete, the sacrificial layer was melted and removed, leaving enclosed microfluidic channels. To avoid channel deformation, an excessive solvent absorption can also be prevented by using a very short solvent exposure times [88].

1.2.2.2.3. Adhesive bonding

Due to the simplicity of adhesive bonding, this approach has been widely used for sealing thermoplastic microfluidic chips. One of the simplest adhesive bonding techniques is by using of glues such as liquid adhesive that set through the evaporation of solvent, or epoxies and acrylates that polymerize and crosslink after mixing with a

catalyzing agent. Commonly, adhesive bonding is performed by applying a thin layer of a high viscosity liquid adhesive which can be cured upon UV light irradiation.

1.2.2.2.4. Other bonding techniques

In 2004, Lei *et al.* employed a microwave-based technique for the precise, localized, low-temperature bonding of PMMA microfluidic devices [89]. Microwave power can be absorbed by a very thin film metal layer deposited on PMMA surface. The intense thin-film volumetric heating promotes localized melting of refractory metals such as gold. One of the advantages of the process is that PMMA is relatively transparent to microwave. Laser welding has also been used to achieve localized sealing of microfluidic chips. A laser beam is focused to heat the plastic at the interface where localized high resolution bonding can be achieved. In addition, flat PDMS films have also been employed to form conformal seal on the plastic microchannels [90].

1.3. References

1.   Crano, J.C. and R.J. Guglielmetti, *Organic photochromic and thermochromic compounds*. Topics in applied chemistry. 1999, New York: Kluwer Academic/Plenum Publishers.

2.   Ercole, F., T.P. Davis, and R.A. Evans, *Photo-responsive systems and biomaterials: photochromic polymers, light-triggered self-assembly, surface*

modification, fluorescence modulation and beyond. Polymer Chemistry, 2010. **1**(1): p. 37-54.

3.   Kato, N., et al., *In Situ Observation of the Thermochromic Phase Transition of the Merocyanine J-Aggregates Monolayer at the Air-Water Interface Using External Infrared Reflection Absorption Spectroscopy.* The Journal of Physical Chemistry B, 2003. **107**(43): p. 11917-11923.

4.   Mishra, A., et al., *Cyanines during the 1990s: A Review.* Chemical Reviews, 2000. **100**(6): p. 1973-2012.

5.   Kimura, K., et al., *Cation complexation, photochromism, and aggregation of copolymers carrying crown ether and spirobenzopyran moieties at the side chains.* Bulletin of the Chemical Society of Japan, 2003. **76**(1): p. 209-215.

6.   Nakatsuji, S., et al., *Novel photo-responsive organic spin systems: preparation and properties of norbornadienes and spiropyrans with TEMPO radical substituents.* Journal of the Chemical Society-Perkin Transactions 2, 2000(9): p. 1969-1975.

7.   Benniston, A.C., et al., *Opening a spiropyran ring by way of an exciplex intermediate.* Journal of Organic Chemistry, 2007. **72**(3): p. 888-897.

8.   Botrel, A., et al., *A theoretical investigation of solvatochromism. Application to merocyanines similar to colored forms obtained by flash-photolysis of spiropyrans.* Chemical Physics, 1995. **194**(1): p. 101-116.

9.   Matsumoto, M., et al., *Light-induced J-aggregation of merocyanine in Langmuir and Langmuir-Blodgett films.* Journal of Physical Chemistry B, 2002. **106**(44): p. 11487-11491.

10.   Delaire, J.A. and K. Nakatani, *Linear and Nonlinear Optical Properties of Photochromic Molecules and Materials.* Chemical Reviews, 2000. **100**(5): p. 1817-1846.

11.   Berkovic, G., V. Krongauz, and V. Weiss, *Spiropyrans and Spirooxazines for Memories and Switches.* Chemical Reviews, 2000. **100**(5): p. 1741-1754.

12.   Abe, S., et al., *Remarkable electric field effect on the absorption intensity of a molecular aggregate of photomerocyanine in a PMMA polymer film.* Chemistry Letters, 1999(2): p. 165-166.

13.   Plaza, P., et al., *Reversible bulk photorelease of strontium ion from a crown ether-linked merocyanine.* Chemphyschem, 2002. **3**(8): p. 668-674.

14.   Onai, Y., et al., *COLORED MEROCYANINE AGGREGATES - LONG-LIVED CRYSTALS OF LARGE-SIZE (10-100-MU-M) AND DEAGGREGATION OF SMALL AGGREGATES IN SOLUTIONS.* Journal of Physical Chemistry, 1993. **97**(37): p. 9499-9505.

15.   Garcia, A., et al., *Photo-, thermally, and pH-responsive microgels.* Langmuir, 2007. **23**(1): p. 224-229.

16.   Winkler, J.D., C.M. Bowen, and V. Michelet, *Photodynamic Fluorescent Metal Ion Sensors with Parts per Billion Sensitivity.* Journal of the American Chemical Society, 1998. **120**(13): p. 3237-3242.

17.   Benniston, A.C. and J. Fortage, *Selenospiropyrans incorporating appended pyrene chromophores.* Tetrahedron Letters, 2008. **49**(27): p. 4292-4295.

18.   Kinashi, K., Y. Harada, and Y. Ueda, *Thermal stability of merocyanine form in spiropyran/silica composite film.* Thin Solid Films, 2008. **516**(9): p. 2532-2536.

19.   Benard, S., et al., *Interplay between magnetism and photochromism in spiropyran-MnPS3 intercalation compounds.* Chemistry of Materials, 2001. **13**(10): p. 3709-3716.

20.   Bouas-Laurent, H. and H. Dürr, *Organic photochromism (IUPAC Technical Report).* Pure and Applied Chemistry, 2001. **73**(4): p. 639-665.

21.   Di Benedetto, F., et al., *Photoswitchable organic nanofibers.* Advanced Materials, 2008. **20**(2): p. 314-+.

22.   Fries, K., et al., *Reversible colorimetric ion sensors based on surface initiated polymerization of photochromic polymers.* Chemical Communications, 2008(47): p. 6288-6290.

23.   Roxburgh, C.J., P.G. Sammes, and A. Abdullah, *Photoreversible Zn2+ Ion Transportation Across an Interface Using Ion-Chelating Substituted*

Photochromic 3,3 '-Indolospirobenzopyrans: Steric and Electronic Controlling Effects. European Journal of Inorganic Chemistry, 2008(31): p. 4951-4960.

24.   Shao, N., et al., *Spiropyran-based fluorescent probes for biological species.* Luminescence, 2008. **23**(2): p. 91-91.

25.   George, M.C., et al., *Direct Laser Writing of Photoresponsive Colloids for Microscale Patterning of 3D Porous Structures.* Advanced Materials, 2009. **21**(1): p. 66-70.

26.   Yagi, S., et al., *Colorimetric sensing of metal ions by bis(spiropyran) podands: Towards naked-eye detection of alkaline earth metal ions.* Dyes and Pigments, 2009. **80**(1): p. 98-105.

27.   Heiligman-Rim, R., Y. Hirshberg, and E. Fischer, *PHOTOCHROMISM IN SPIROPYRANS. PART V.1 ON THE MECHANISM OF PHOTOTRANSFORMATION.* The Journal of Physical Chemistry, 1962. **66**(12): p. 2470-2477.

28.   Gorner, H., *Photoprocesses in spiropyrans and their merocyanine isomers: Effects of temperature and viscosity.* Chemical Physics, 1997. **222**(2-3): p. 315-329.

29.   Chibisov, A.K. and H. Gorner, *Photoprocesses in spiropyran-derived merocyanines.* Journal of Physical Chemistry A, 1997. **101**(24): p. 4305-4312.

30.   Yagi, S., K. Maeda, and H. Nakazumi, *Photochromic properties of cationic merocyanine dyes. Thermal stability of the spiropyran form produced by irradiation with visible light.* Journal of Materials Chemistry, 1999. **9**(12): p. 2991-2997.

31.   Chibisov, A.K. and H. Gorner, *Singlet versus triplet photoproceses in indodicarbocyanine dyes and spiropyran-derived merocyanines.* Journal of Photochemistry and Photobiology a-Chemistry, 1997. **105**(2-3): p. 261-267.

32.   Gorner, H., *Photochemical ring opening in nitrospiropyrans: triplet pathway and the role of singlet molecular oxygen.* Chemical Physics Letters, 1998. **282**(5-6): p. 381-390.

33.   Haupl, T., et al., *The Competitive Effect of Intramolecular Charge Transfer on the Photochromism of Spiro[cyclohexadiene-indolines] Studied by ps-Spectroscopy.* The Journal of Physical Chemistry A, 1999. **103**(35): p. 6904-6910.

34.   Hobley, J., et al., *Proton exchange and isomerisation reactions of photochromic and reverse photochromic spiro-pyrans and their merocyanine forms.* Physical Chemistry Chemical Physics, 1999. **1**(14): p. 3259-3267.

35.   Bouas-Laurent, H., et al., *Organic Photochromism*, in *Photochromism*. 2003, Elsevier Science: Amsterdam. p. XXVII-LIII.

36. Tanaka, M., et al., *Synthesis and photochromism of spirobenzopyran derivatives bearing an oxymethylcrown ether moiety: Metal ion-induced switching between positive and negative photochromisms.* Journal of Organic Chemistry, 2001. **66**(5): p. 1533-1537.

37. Byrne, R. and D. Diamond, *Chemo/bio-sensor networks.* Nature Materials, 2006. **5**(6): p. 421-424.

38. Crano, J.C., et al., *Photochromic compounds: Chemistry and application in ophthalmic lenses.* Pure and Applied Chemistry, 1996. **68**(7): p. 1395-1398.

39. Raymo, F.M. and S. Giordani, *All-optical processing with molecular switches.* Proceedings of the National Academy of Sciences of the United States of America, 2002. **99**(8): p. 4941-4944.

40. Radu, A., et al., *Photonic modulation of surface properties: a novel concept in chemical sensing.* Journal of Physics D-Applied Physics, 2007. **40**(23): p. 7238-7244.

41. Kelly, J.M., C.B. McArdle, and M.J.d.F. Maunder, *Photochemistry and Polymeric Systems*. Photochromic organic compounds in polymer matrices, ed. J.C. Crano, et al. 1993, Cambridge: Royal Society of Chemistry. 179-193.

42. Bertelson, R.C., *REMINISCENCES ABOUT ORGANIC PHOTOCHROMICS.* Molecular Crystals and Liquid Crystals Science and Technology Section a-Molecular Crystals and Liquid Crystals, 1994. **246**: p. 1-8.

43.   Evans, L., et al., *Selective Metals Determination with a Photoreversible Spirobenzopyran.* Analytical Chemistry, 1999. **71**(23): p. 5322-5327.

44.   Collins, G.E., et al., *Photoinduced switching of metal complexation by quinolinospiropyranindolines in polar solvents.* Chemical Communications, 1999(4): p. 321-322.

45.   Leaustic, A., et al., *Photochromism of cationic spiropyran-doped silica gels.* New Journal of Chemistry, 2001. **25**(10): p. 1297-1301.

46.   Shao, N., et al., *Copper ion-selective fluorescent sensor based on the inner filter effect using a spiropyran derivative.* Analytical Chemistry, 2005. **77**(22): p. 7294-7303.

47.   Inouye, M., et al., *Alkali metal recognition induced isomerization of spiropyrans.* Journal of the American Chemical Society, 1990. **112**(24): p. 8977-8979.

48.   Tian, Z.Y., et al., *Single-Chromophore-Based Photoswitchable Nanoparticles Enable Dual-Alternating-Color Fluorescence for Unambiguous Live Cell Imaging.* Journal of the American Chemical Society, 2009. **131**(12): p. 4245-4252.

49.   Kinashi, K., et al., *Multi-photochromic behavior of hybrid material with spirobenzopyran and azobenzene moieties.* Chemistry Letters, 2006. **35**(3): p. 298-299.

50. Kimura, K., T. Teranishi, and M. Yokoyama, *Highly calcium-ion-accelerated coloration of bis(spirobenzopyran) bridged by diaza-18-crown-6 moiety at the 8-position.* Supramolecular Chemistry, 1996. **7**(1): p. 11-13.

51. Kimura, K., H. Sakamoto, and T. Nakamura, *Application of photoresponsive polymers carrying crown ether and spirobenzopyran side chains to photochemical valve.* Journal of Nanoscience and Nanotechnology, 2006. **6**(6): p. 1741-1749.

52. Kimura, K., M. Sumida, and M. Yokoyama, *Drastic metal-ion enhancement in photoinduced aggregation of copolymers carrying crown ether and spirobenzopyran moieties.* Chemical Communications, 1997(15): p. 1417-1418.

53. Shao, N., et al., *Design of Bis-spiropyran Ligands as Dipolar Molecule Receptors and Application to in Vivo Glutathione Fluorescent Probes.* Journal of the American Chemical Society, 2010. **132**(2): p. 725-736.

54. Tomizaki, K.Y., X. He, and H. Mihara, *A chromism-based assay (CHROBA) technique for in situ detection of protein kinase activity.* Bioorganic & Medicinal Chemistry Letters, 2005. **15**(6): p. 1731-1735.

55. Tomizaki, K. and H. Mihara, *PHOTOCHROMIC SPIROPYRAN-CONTAINING PEPTIDES FOR A NOVEL PROTEIN DETECTING SYSTEM.* Journal of Peptide Science, 2004. **10**: p. 158-158.

56.   Manz, A., et al., *Micromachining of monocrystalline silicon and glass for chemical analysis systems A look into next century's technology or just a fashionable craze?* TrAC Trends in Analytical Chemistry, 1991. **10**(5): p. 144-149.

57.   Jacobson, S.C., et al., *Effects of Injection Schemes and Column Geometry on the Performance of Microchip Electrophoresis Devices.* Analytical Chemistry, 1994. **66**(7): p. 1107-1113.

58.   Harrison, D.J., et al., *Capillary electrophoresis and sample injection systems integrated on a planar glass chip.* Analytical Chemistry, 1992. **64**(17): p. 1926-1932.

59.   Kikutani, Y., et al., *Glass microchip with three-dimensional microchannel network for 2 [times] 2 parallel synthesis.* Lab on a Chip, 2002. **2**(4): p. 188-192.

60.   Kikutani, Y., et al., *Pile-up glass microreactor.* Lab on a Chip, 2002. **2**(4): p. 193-196.

61.   Wang, H.Y., et al., *Low temperature bonding for microfabrication of chemical analysis devices.* Sensors and Actuators B: Chemical, 1997. **45**(3): p. 199-207.

62.   Akiyama, Y., et al., *Rapid bonding of Pyrex glass microchips.* Electrophoresis, 2007. **28**(6): p. 994-1001.

63. Wallis, G., *DIRECT-CURRENT POLARIZATION DURING FIELD-ASSISTED GLASS-METAL SEALING.* Journal of the American Ceramic Society, 1970. **53**(10): p. 563-&.

64. Sayah, A., et al., *Development of novel low temperature bonding technologies for microchip chemical analysis applications.* Sensors and Actuators A: Physical, 2000. **84**(1-2): p. 103-108.

65. Chiem, N., et al., *Room temperature bonding of micromachined glass devices for capillary electrophoresis.* Sensors and Actuators B: Chemical, 2000. **63**(3): p. 147-152.

66. Xia, Y.N. and G.M. Whitesides, *Soft lithography.* Angewandte Chemie-International Edition, 1998. **37**(5): p. 551-575.

67. Xia, Y.N. and G.M. Whitesides, *Soft lithography.* Annual Review of Materials Science, 1998. **28**: p. 153-184.

68. Jeon, N.L., et al., *Fabrication of silicon MOSFETs using soft lithography.* Advanced Materials, 1998. **10**(17): p. 1466-1469.

69. Tsao, C.W. and D.L. DeVoe, *Bonding of thermoplastic polymer microfluidics.* Microfluidics and Nanofluidics, 2009. **6**(1): p. 1-16.

70. Martynova, L., et al., *Fabrication of plastic microfluid channels by imprinting methods.* Analytical Chemistry, 1997. **69**(23): p. 4783-4789.

71.   Xu, J.D., et al., *Room-temperature imprinting method for plastic microchannel fabrication.* Analytical Chemistry, 2000. **72**(8): p. 1930-1933.

72.   McCormick, R.M., et al., *Microchannel electrophoretic separations of DNA in injection-molded plastic substrates.* Analytical Chemistry, 1997. **69**(14): p. 2626-2630.

73.   Giselbrecht, S., et al., *3D tissue culture substrates produced by microthermoforming of pre-processed polymer films.* Biomedical Microdevices, 2006. **8**(3): p. 191-199.

74.   Yuan, D.J. and S. Das, *Experimental and theoretical analysis of direct-write laser micromachining of polymethyl methacrylate by CO2 laser ablation.* Journal of Applied Physics, 2007. **101**(2).

75.   Cheng, J.-Y., et al., *Direct-write laser micromachining and universal surface modification of PMMA for device development.* Sensors and Actuators B: Chemical, 2004. **99**(1): p. 186-196.

76.   Brister, P.C. and K.D. Weston, *Patterned Solvent Delivery and Etching for the Fabrication of Plastic Microfluidic Devices.* Analytical Chemistry, 2005. **77**(22): p. 7478-7482.

77.   Becker, H. and C. Gärtner, *Polymer microfabrication technologies for microfluidic systems.* Analytical and Bioanalytical Chemistry, 2008. **390**(1): p. 89-111.

78. Chen, Q., et al., *Light-Triggered Self-Assembly of a Spiropyran-Functionalized Dendron into Nano-/Micrometer-Sized Particles and Photoresponsive Organogel with Switchable Fluorescence.* Advanced Functional Materials. **20**(1): p. 36-42.

79. Galloway, M., et al., *Contact Conductivity Detection in Poly(methyl methacylate)-Based Microfluidic Devices for Analysis of Mono- and Polyanionic Molecules.* Analytical Chemistry, 2002. **74**(10): p. 2407-2415.

80. Chen, Z., et al., *Vacuum-assisted thermal bonding of plastic capillary electrophoresis microchip imprinted with stainless steel template.* Journal of Chromatography A, 2004. **1038**(1-2): p. 239-245.

81. Kelly, R.T. and A.T. Woolley, *Thermal Bonding of Polymeric Capillary Electrophoresis Microdevices in Water.* Analytical Chemistry, 2003. **75**(8): p. 1941-1945.

82. Klank, H., J.P. Kutter, and O. Geschke, *CO2-laser micromachining and back-end processing for rapid production of PMMA-based microfluidic systems.* Lab on a Chip, 2002. **2**(4): p. 242-246.

83. Yussuf, A.A., et al., *Sealing of polymeric-microfluidic devices by using high frequency electromagnetic field and screen printing technique.* Journal of Materials Processing Technology, 2007. **189**(1-3): p. 401-408.

84. Tennico, Y.H., et al., *Surface modification-assisted bonding of polymer-based microfluidic devices.* Sensors and Actuators B-Chemical, 2010. **143**(2): p. 799-804.

85. Rahbar, M., et al., *Microwave-induced, thermally assisted solvent bonding for low-cost PMMA microfluidic devices.* Journal of Micromechanics and Microengineering, 2010. **20**(1).

86. Koesdjojo, M.T., C.R. Koch, and V.T. Remcho, *Technique for Microfabrication of Polymeric-Based Microchips from an SU-8 Master with Temperature-Assisted Vaporized Organic Solvent Bonding.* Analytical Chemistry, 2009. **81**(4): p. 1652-1659.

87. Kelly, R.T., T. Pan, and A.T. Woolley, *Phase-changing sacrificial materials for solvent bonding of high-performance polymeric capillary electrophoresis microchips.* Analytical Chemistry, 2005. **77**(11): p. 3536-3541.

88. Griebel, A., et al., *Integrated polymer chip for two-dimensional capillary gel electrophoresis.* Lab on a Chip, 2004. **4**(1): p. 18-23.

89. Lei, K.F., et al., *Microwave bonding of polymer-based substrates for potential encapsulated micro/nanofluidic device fabrication.* Sensors and Actuators A: Physical, 2004. **114**(2-3): p. 340-346.

90. Barker, S.L.R., et al., *Plastic Microfluidic Devices Modified with Polyelectrolyte Multilayers.* Analytical Chemistry, 2000. **72**(20): p. 4899-4903.

CHAPTER 2

PHOTOACTIVABLE RESINS FOR LEAD ION EXTRACTION

Jintana Nammoonnoy, Jeffrey R. Walker, and Vincent T. Remcho

Department of Chemistry, Oregon State University, Corvallis, OR 97330 USA

2.1. Abstract

A novel approach to heavy metal extraction from drinking water using spiropyran-modified resins is presented. Spiropyrans are metal chelating ligands used in the process of photoreversible complexation. Spiro compounds are a well-known class of dyes that exhibit interesting photochromic functionality in that their structure changes reversibly with UV/visible irradiation. The photoinduced process of spiropyran involves the cleavage of the spiro carbon-oxygen bond upon UV light irradiation and subsequent isomerization to its open form. Spiropyran chemistry found its application in heavy metal ion extraction by first chelating the ions (after the spiro compound is activated using UV light). Subsequently, the contaminants are released when the metal-spiropyran complex is exposed to visible light. In this work the retention and release of metal ions on the spiropyran-modified stationary phase is controlled by UV/visible irradiation. The extraction of Pb^{2+} ions from an aqueous solution using immobilized spiropyrans resins is studied. We demonstrate that spiropyrans retain their photochromic properties when immobilized on the surface of the resins and can successfully perform Pb^{2+} extractions from aqueous solution.

2.2. PHOTOACTIVABLE RESINS FOR LEAD ION EXTRACTION

Spiropyran derivatives have been immobilized on the surfaces of resins using various immobilization strategies. These functionalized resins can be reversibly switched between the inactive spiropyran (SP) and the more polar merocyanine (MC) form using low power light sources, such as light emitting diodes (LEDs). A UV LED array (390 nm) is used for the SP $\rightarrow$MC conversion, and a green LED array (525 nm) for the reverse MC $\rightarrow$ SP conversion. The spiropyran coated resins have been characterized using IR spectroscopy. Application of spiropyran functionalized resins for lead ion (Pb^{2+}) extraction has been investigated. Investigations into the Pb^{2+} binding behavior of the spiropyran modified resins has shown that the concentration of Pb^{2+} changed upon UV irradiation during the extraction process, suggesting that a significant and reversible interaction between Pb^{2+} and MC is occurring. The Pb^{2+} ions can be completely released by photonic conversion of the resins into the inactive SP form using the green LED array. This extraction sequence has been successfully repeated three times, suggesting that it is possible to cycle through activation of the functionalized resins from the non-binding form to the binding form (SP $\rightarrow$ MC) using the UV LED array, to allow binding with Pb^{2+} ions to occur, and, subsequently, to release the bound ions and regenerate the passive SP surface using the green LED array. The system can therefore form the basis of a photoactivable stationary phase for metal ion extraction: irradiation of the stationary phase with UV LEDs causes retention of guest species due to the presence of MC form, while subsequent exposure to green LEDs leads to release of the guest species into the mobile phase.

The removal of metals from water is important in a number of environmental and industrial applications. Conventional metal removal techniques involve complexation or ion exchange. Although these technologies are effective and well-established, there are problems associated with them. One such problem is that complexation requires the use of organic ligands which often cannot be reused. In addition, ion exchange requires heat or caustics to regenerate the resins. Therefore, there is ongoing interest in the development of reversible metal-chelation agents in which chelation can be switched on and off by exposure to light of different wavelengths. Popular substrates for such studies are the spiropyran system and its analogues since these have well-documented photochromical properties. Spiropyrans are organic photochromic compounds that have been widely studied [1-5]. They are composed of two heterocyclic parts linked together by a tetrahedral sp^3 spiro carbon atom. Irradiation of a spiropyran with UV light induces heterolytic cleavage of the spiro carbon-oxygen bond, producing the open form of the ring, the intensely colored merocyanine (Figure 2.1).
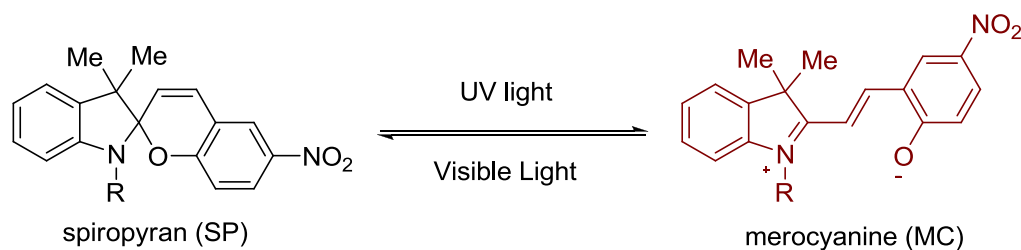
Figure 2.1 Photoconversion of spiropyran to merocyanine.

Metal ions can influence this isomerization process by associating with the open form through the electron-rich oxygen atom. In contrast, visible light produces a high concentration of the closed form, and thus hinders metal-binding. Spiropyrans, therefore, show great potential as photo-reversible metal-complexation agents. This spiropyran chemistry is applicable to extraction of metal ions by first chelating the ions by using UV light, and subsequently exposing the metal-spiropyran complex to visible light to elute contaminants efficiently in a concentrated plug (Figure 2.2).
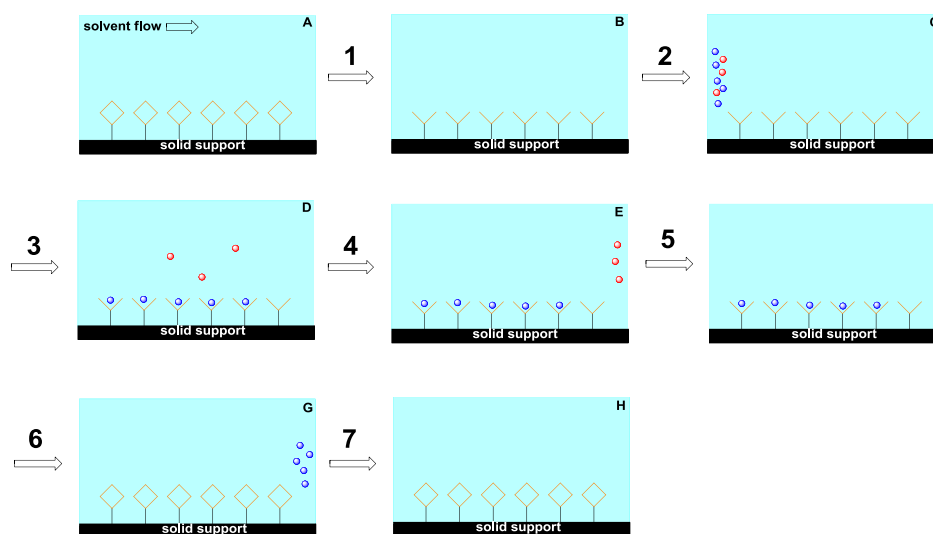
Figure 2.2 Semi-continuous extraction of heavy metal ions generates a continuous stream of purified water; non-binding form (⬦), binding form (∨), targeted metal ions (🔵), non-targeted metal ions (🔴).

This process can be used in environmental and industrial processes to remove metals from aqueous solutions. The metals are released from the ligands upon irradiation with visible light. The regeneration of the ligands and concentration of metals is likely to be more facile than is the case with conventional ion exchange resins. The use of light to trigger the chelator offers unique opportunities that

minimize waste generation and power requirements. Advances in the integration of LED (light emitting diode) sources in the system hold promise for the production of low cost miniaturized systems.

Interest in this application arises because it provides a means to trigger metal ion binding and release without addition of any auxiliary reagents. We report herein on the unique properties of spiropyrans for water reclamation using light to gate metal ion capture and release. Since lead (Pb^{2+}) is widely distributed in nature and given its adverse effects on human health, it was selected as a model divalent metal cation for the extraction study.

Initially, spiropyran derivatives were synthesized using previously reported procedures [6, 7]. Placing a nitro group at position R´ (Figure 2.3) stabilized the open form of the spiropyran. Further, the addition of an electron donor group on at position L generates an auxiliary ligating group [8].
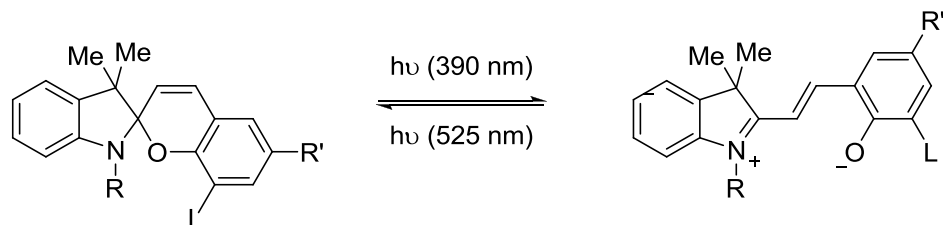
1a R=CH$_3$, R´= H, L = OH

1b R=C$_3$H$_6$COOH, R´= NO$_2$, L´= H

1c R=C$_3$H$_6$COOH, R´= NO$_2$, L´= OCH$_3$

Figure 2.3 Light-modulated transformation from spiropyran (SP) to merocyanine (MC).

We have designed spiropyran derivatives incorporating a methoxy moiety at the 8-position in which cation-binding enhancement is expected on photoisomerization to the corresponding merocyanine form. Sterically-favorable cooperation of the resulting phenolate anion together with the methoxy moiety provides a suitable chelator for cation. Actually, a powerful interaction between the phenolate anion and methoxy-complexed metal ions, especially lead ions, was found in the merocyanine isomer spiropyran. Spiropyrans were then allowed to react with Merrifield resins or aminate polystyrene resins via carbodiimide coupling protocols (Figure 2.4) to yield a convenient resin for extraction studies.

1. EDC, CH_2Cl_2. **2**. 50% TFA, CH_2Cl_2. **3**. SP, EDC, CH_2Cl_2.
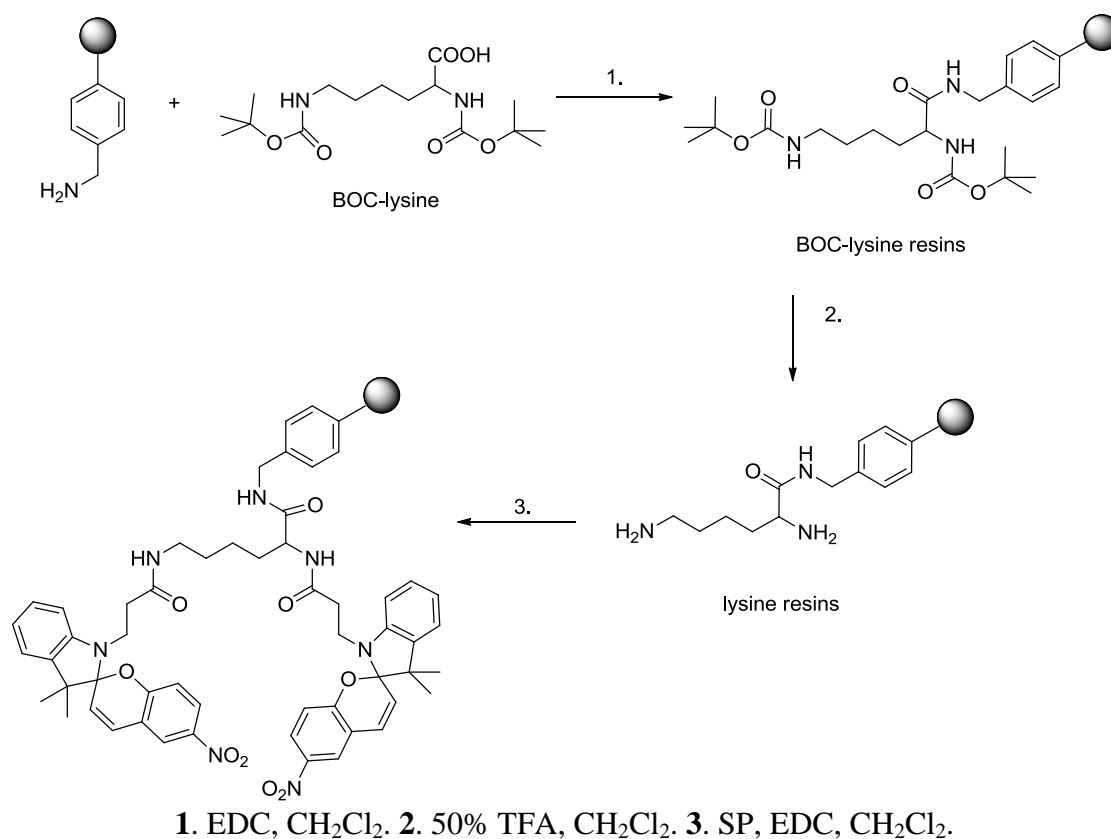
Figure 2.4 Schematic of the synthesis of photochromic resins.

Changes in the UV absorption spectra of SP-MC in dichloromethane under irradiation with UV light of λ = 365 nm and then subsequently with visible light of λ = 525 nm were examined. Figure 2.5 shows the measured UV absorption of SP-MC in dichloromethane after irradiation with UV light for 5 min and subsequently with visible light for 5 min. A new absorption peak is found to appear at 526 nm in the spectrum on irradiation with UV light, and is assigned to the merocyanine form. The peak disappears under consequent irradiation with visible light, and the spectrum returns almost completely to the original one.
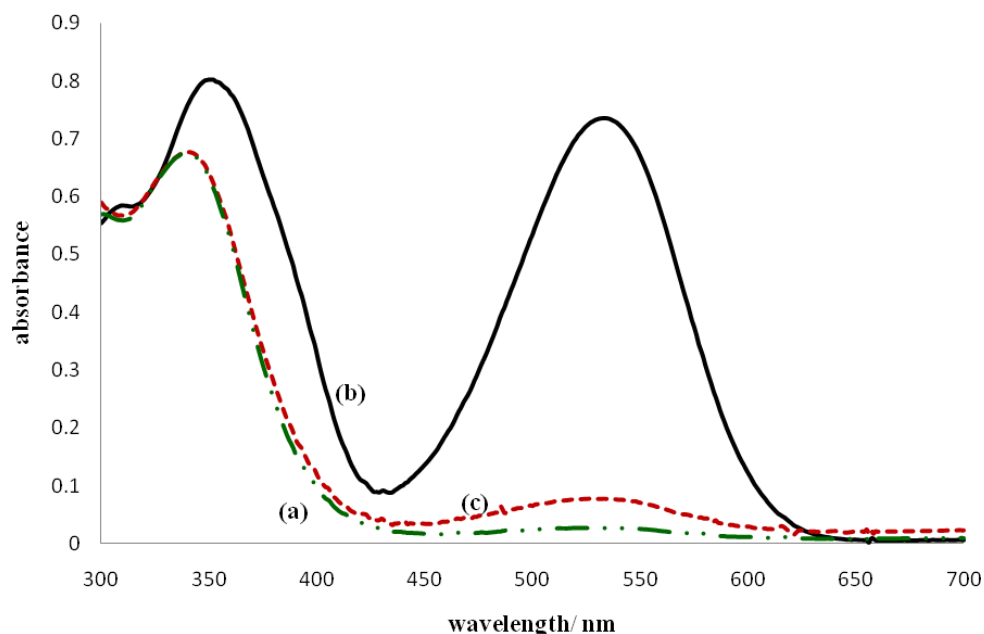
Figure 2.5 Changes in the UV absorption spectrum of SP-MC in dichloromethane under irradiation with UV light of λ = 365 nm and subsequently with visible light of λ = 525 nm. (a) before irradiation; (b) after irradiation with UV light for 5 min; (c) after subsequent irradiation with visible light for 5 min; [SP-MC] = 1×10^{-4} mol/L.

The SP-MC resins were also characterized by IR spectroscopy. Figure 2.6 shows the IR absorption spectra of aminated polystyrene resins, Boc-lysine resins, lysine resins, Bis-SP-lysine, and Bis-SP-lysine modified resins. An absorption peak at around 1620 cm^{-1}, which is assigned to the C=O stretch of the amide group, in the spectrum of Boc-lysine resins is found to decrease with introduction of the spiropyran moiety. An absorption peak at 1650 cm^{-1} is assigned to the carbonyl group from amide, those at 1500 and 1340 cm^{-1} are assigned to N-O in the nitro group, and a peak at 1100 cm^{-1} is assigned to O-C in the methoxy group. These results confirm the presence of the spiropyran moieties in Bis-spiropyran-lysine resins.
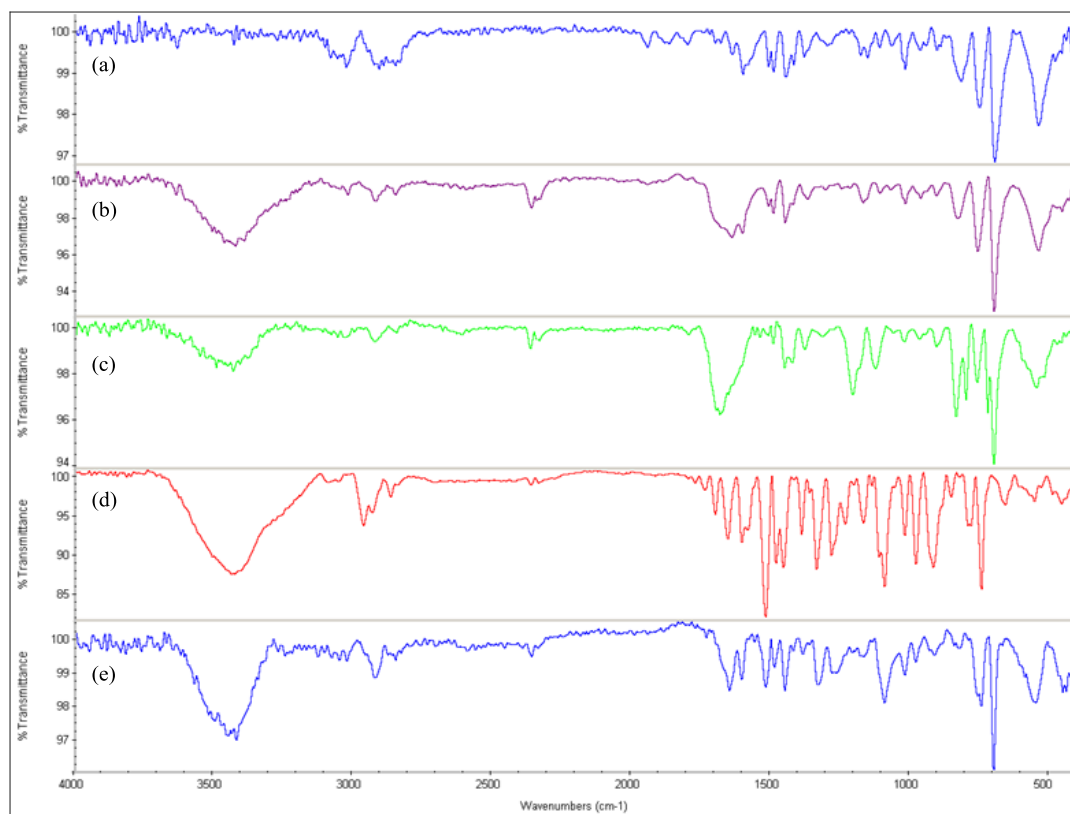
Figure 2.6 IR absorption spectra of (a) Aminated polystyrene resins; (b) BOC-lysine resins; (c) lysine resins; (d) Bis-SP-lysine and (e) Bis-SP-lysine resins.

The spiropyran modified resins showed spectral changes similar to those observed solution phase SP-MC in dichloromethane on irradiation with UV light and subsequently with visible light. The resins turned from red to deep purple after irradiation with UV light, and reverted to red after irradiation with visible light. However, the isomerization rates (especially the disappearance rates of the merocyanine forms) for the resins were slower than was observed in solution (Figure 2.7).

UV (390 nm)

VIS (525 nm)
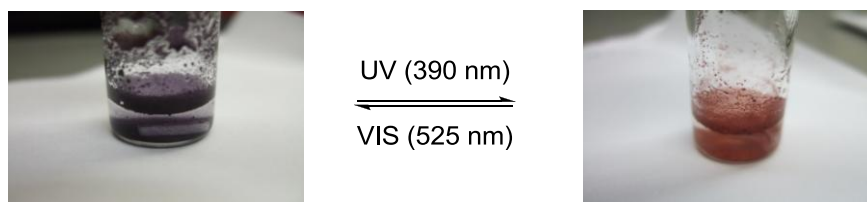
Figure 2.7 The spiropyran modified resins before and after 5 min irradiation with UV light.

Most importantly, these results show that the photoisomerization of spiropyran moieties on the modified resins is reversible. The color change suggests generation of the open form of the spiropyran-modified resin, which then complexes Pb^{2+} ions. The reddish resin reappeared after irradiation with the green LED array. Thus, stabilization of the Pb^{2+}-complexed open form in an extremely polar solvent such as water does not prevent isomerization to the closed form under visible light. Initial screening results suggest that spiropyran modified Merrifield resins can bind with lead ions from solution.

Application of the newly modified spiropyran resins to Pb^{2+} extraction from aqueous solution was done in triplicate. A simple, batch technique was used in order to define optimum conditions including irradiation time. Typically, 20 mg of modified resins were packed in a home-built resin cartridge as shown in Figure 2.8.
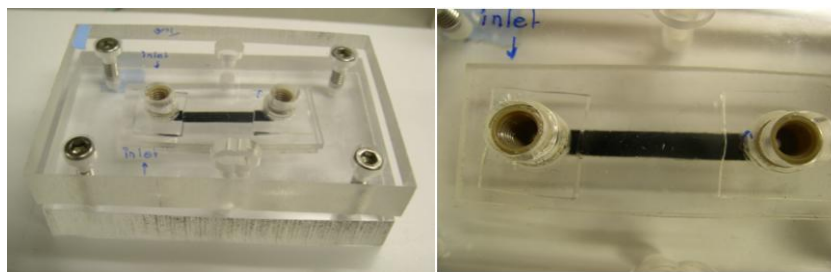
Figure 2.8 In-house-designed resin cartridge consisting of a clamped device equipped with Upchurch nanoports for fluidic connections, PMMA chip which contains a thin layer of spiropyran-functionalized resin.

A Pb^{2+} solution containing 50 ppb Pb^{2+} was flowed through the resin bed at 20 µL/min using a peristaltic pump, described as follows:

1. Start flow of Pb^{2+} solution at 20 µL/min.

2. Activate UV exposure (390 nm) for 30 min.

3. Collect fractions of solution at 20 second intervals for measuring Pb^{2+} quantifications via ICP-MS.

Following the experiments, the free unextracted Pb^{2+} concentration was plotted as a function of UV irradiation time as shown in Figure 2.9. The Pb^{2+} content decreased with increasing the UV irradiation time, reaching the lowest value at 5 min irradiation followed by an increasing in Pb^{2+} content beyond 5 min. Therefore, the adsorption of Pb^{2+} was effective at 5 min UV irradiation.
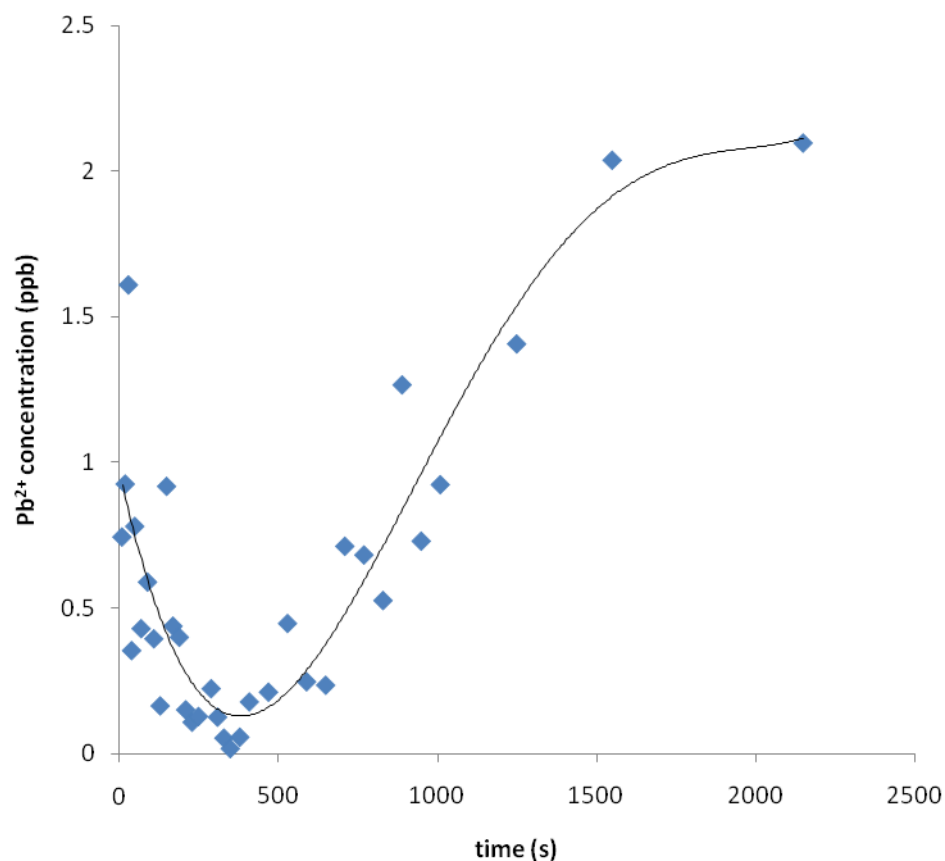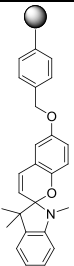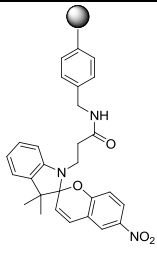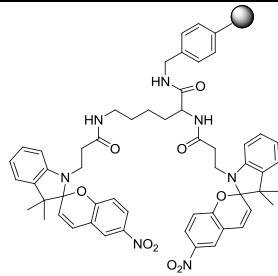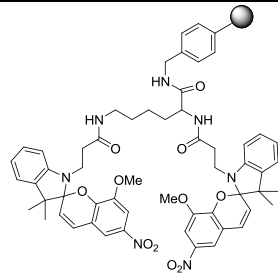
Figure 2.9 Pb^{2+} concentrations recorded during UV LED irradiation (390 nm) showing that the most effective irradiation time for binding Pb^{2+} ions is 5 min.

The efficiency of the modified resin is an important factor to indicate the effects of substituent groups on spiropyran ring on Pb^{2+} extraction. The loading capacity was determined at optimum UV irradiation time which was 5 min and the results expressed in the percentage of Pb^{2+} extraction. The percentage of Pb^{2+} sorption was calculated by measuring the Pb^{2+} content before and after the chelation. The percentage of sorption increased from 2 to 7% with more stable MC form (SP2), as shown in Table 2.1. The amount of spiropyran molecules is increased by using lysine as a spacer (SP3) resulting in an increase in the Pb^{2+} uptake to 10 folds as compared to

SP1. A comparison between the Pb^{2+} uptake values of SP3 and SP4 indicates an appreciated increase from 20 to 91 due to the contribution of the methoxy ligating moiety in metal binding.

Table 2.1 Efficiencies of spiropyran modified resins for Pb^{2+} extraction with 5 min UV irradiation.

Modified resins	SP1	SP2	SP3	SP4
structure				
% Pb^{2+} extraction	2.09	7.50	20.00	91.24

In conclusion, we have demonstrated photoreversible Pb^{2+} extraction using spiropyran modified resins. Upon exposure to appropriate stimuli, these resins display photo-controlled uptake and release of certain metal ions. Increase in Pb^{2+} loading capacity was observed by replacing a functional group on spiropyran ring. Further studies directed toward the structural modification of the spiropyran molecule to allow us to trap Pb^{2+} more efficiently and with greater specificity are currently underway in our laboratory.

2.3. Acknowledgement

2.4. References

1.   Cabrera, I., V. Krongauz, and H. Ringsdorf, *PHOTOCHROMIC AND THERMOCHROMIC LIQUID-CRYSTAL POLYMERS WITH SPIROPYRAN GROUPS.* Molecular Crystals and Liquid Crystals, 1988. **155**: p. 221-230.

2.   Unuma, Y. and A. Miyata, *LIGHT-INDUCED MOLECULAR-ORIENTATION IN LANGMUIR-BLODGETT-FILMS OF SPIROPYRAN.* Sharp Technical Journal, 1989(43): p. 45-50.

3.   Pigois, E., et al., *X-RAY PHOTOELECTRON-SPECTROSCOPY OF SPIROPYRAN MOLECULES.* Journal of Electron Spectroscopy and Related Phenomena, 1990. **53**(1-2): p. 79-86.

4.   Kuhn, D., H. Balli, and U.E. Steiner, *KINETIC-STUDY OF THE PHOTODECOLORATION MECHANISM OF AN INVERSELY PHOTOCHROMIC CLASS OF COMPOUNDS FORMING SPIROPYRAN ANALOGS.* Journal of Photochemistry and Photobiology a-Chemistry, 1991. **61**(1): p. 99-112.

5.   Rappon, M., et al., *PHOTOINDUCED REACTION OF DYE IN POLYMER MEDIA .1. UNANNEALED POLYMER MATRICES.* European Polymer Journal, 1991. **27**(4-5): p. 365-370.

6.   Garcia, A.A., et al., *Photon-controlled phase partitioning of spiropyrans.* Journal of Physical Chemistry A, 2000. **104**(26): p. 6103-6107.

7.   Raymo, F.M. and S. Giordani, *All-optical processing with molecular switches.* Proceedings of the National Academy of Sciences of the United States of America, 2002. **99**(8): p. 4941-4944.

8.   Winkler, J.D., K. Deshayes, and B. Shao, *Photodynamic transport of metal ions.* Journal of the American Chemical Society, 1989. **111**(2): p. 769-770.

CHAPTER 3

A PHOTOACTIVABLE MICROFLUIDIC DEVICE FOR LEAD ION

EXTRACTION

Jintana Nammoonnoy, Jeffrey R. Walker, and Vincent T. Remcho

Department of Chemistry, Oregon State University, Corvallis, OR 97331

3.1 Abstract

We have investigated the beneficial characteristics of microfluidic devices and spiropyran dyes to produce a simple and innovative microchip for photo-controlled Pb^{2+} ion extraction, configured as an automated metal ion accumulation and release. The microfluidic device consists of channels with a depth of 50 μm and width of 100 μm fabricated in polymethylmethacrylate (PMMA). A custom spiropyran is immobilized covalently to the oxygen plasma treated PMMA micro-channel walls. When the colorless and inactive spiropyran coating absorbs UV light, it reconfigures to the colored merocyanine form, which also has an active binding site for certain metal ions. Therefore, metal ion uptake can be triggered using UV light and subsequently reversed on demand by shining visible light on the colored complex, which regenerates the inactive spiropyran form and releases the metal ion. Following photoactivation of spiropyran in the microchip, lead ion (Pb^{2+}) was successfully extracted from solution and recaptured from the chip upon visible light exposure.

3.2. Introduction

The removal of metals from aqueous solution is important in a number of environmental and industrial applications. Conventional techniques to remove metal ions involve complexation or ion exchange. While these technologies are effective and well-established, there are problems associated with them. Complexation requires the use of organic ligands, which often cannot be reused, and ion exchange requires heat or caustics to regenerate the resins. We have been studying the use of an alternative material that photoactivates to adsorb metal ions and can be easily regenerated with

visible light. Because of the absorption spectra of photoactivable materials overlap with the solar spectrum, these materials can be activated and regenerated using solar radiation.

We have been investigating the use of a spiropyran as a photoactivated ion exchange material. Spiropyrans are organic photochromic compounds that have been widely studied. Upon irradiation with UV or visible light, spiropyrans isomerize between neutral (closed form SP) define SP and zwitterionic (open form) structures, in which the open form is comparatively more polar. Metal ions can influence this isomerization process by associating with the UV-induced open form through the electron-rich oxygen atom. In contrast, visible light produces a high concentration of the closed form, and thus hinders metal-binding. Spiropyrans, therefore, show great potential as photo-reversible metal-complexation agents. A number of interesting systems have been developed displaying photodynamic transport [1].

Figure 3.1 illustrates the use of photochromic dyes as light activated binders of metal ions. This process can be used in environmental and industrial processes to remove metals from aqueous solutions. The metals are released from the ligands upon irradiation with visible light. The regeneration of the ligands is likely to be more facile than is the case with conventional ion exchange resins. Additionally, the use of light to trigger the chelator offers unique opportunities. Advances in the integration of LED

(light emitting diode) sources in the system hold promise for the production of low-cost miniaturized systems.
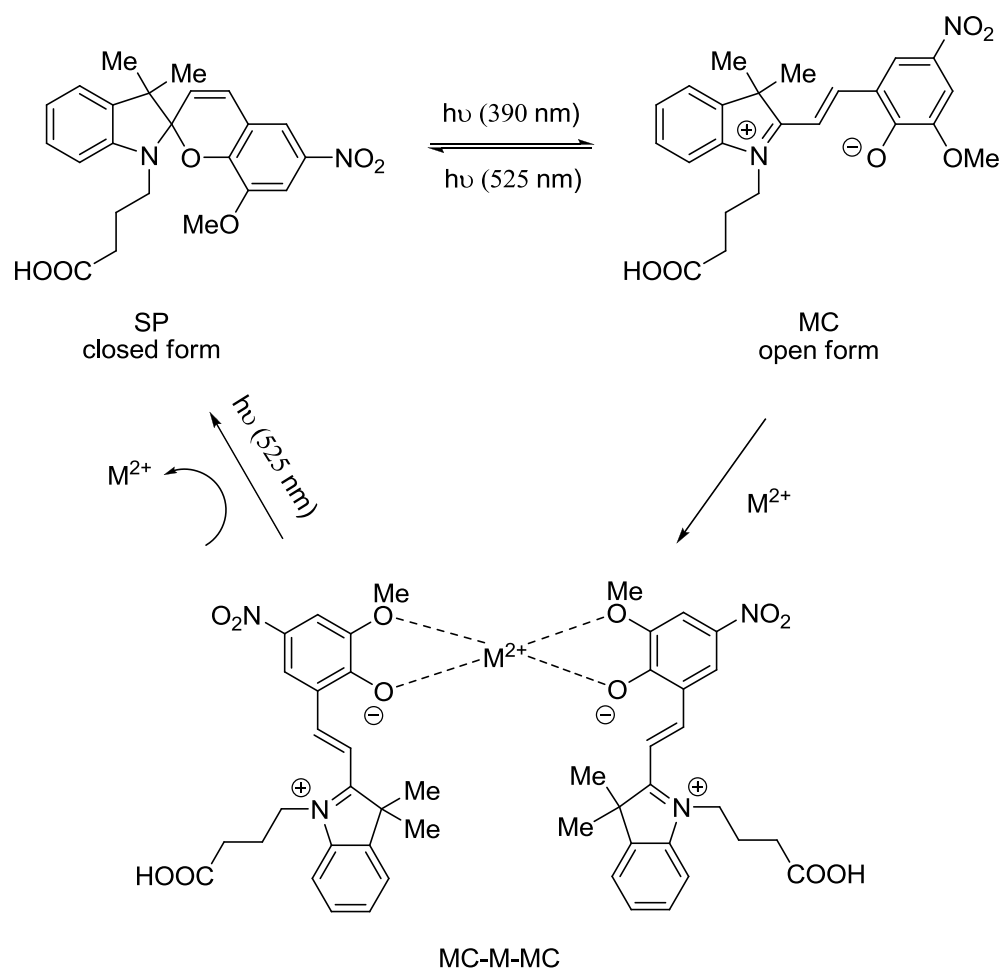
Figure 3.1 Schematic of the light-modulated transformation from spiropyran (SP) to merocyanine (MC). The dimeric complex of MC with metal ions is also shown.

In this paper we show that photochromic spiropyran molecules immobilized to poly(methylmethacrylate) (PMMA) microchannels can successfully serve as a photoactivable extraction system for metal ions. The micro-channels are functionalized by simply flowing solutions of spiropyran through the channels which previously were activated by oxygen plasma treatment. Covalently bound polymer chains of spiropyran allow for extraction stability and provide reversible, switchable binding surfaces. Anchoring lysine molecules to activated PMMA surfaces increases functionality of spiropyran providing the amplification of extraction efficiency of the microchip. As a result, the microchips can be effectively used for heavy ion extraction through either binding or releasing the ions depending on the wavelength of irradiating light.

3.3. Experimental

3.3.1. Materials and instruments

2,3,3-trimethylindolenine, 3-methoxy-5-nitrosalicylaldehyde 4-bromo butyric acid, *N*-(3-dimethylaminopropyl)-*N*´-ethylcarbodiimide (EDC) 1,8-diaminooctane and DL-lysine were purchased from Sigma-Aldrich (Milwaukee, WI, USA) and were used as received. The requisite spiropyran handle, 11´-(3-carboxypropyl)-3,3´-dimethyl-6-nitrospiro-[2H-1]-benzopyran-2,2´-indoline (SP-COOH, Scheme 1) was produced in a

three-step sequence as described elsewhere [2]. Lead perchlorate trihydrate was purchased from MP Biomedical INC. (Solon, OH, USA). UV-vis spectra were recorded on an Agilent 8453UV-vis spectrometer (Santa Clara, CA, USA). The UV irradiation (390 nm LEDs) and visible irradiation (525 nm LEDs) sources were obtained from V-LEDS.com (Bellingham, WA, USA).

3.3.2. Spiropyran Synthesis

Spiropyrans were synthesized in a three-step sequence as shown in Figure 3.2.

R=H, OMe

SPCOOMe

SPCOOH
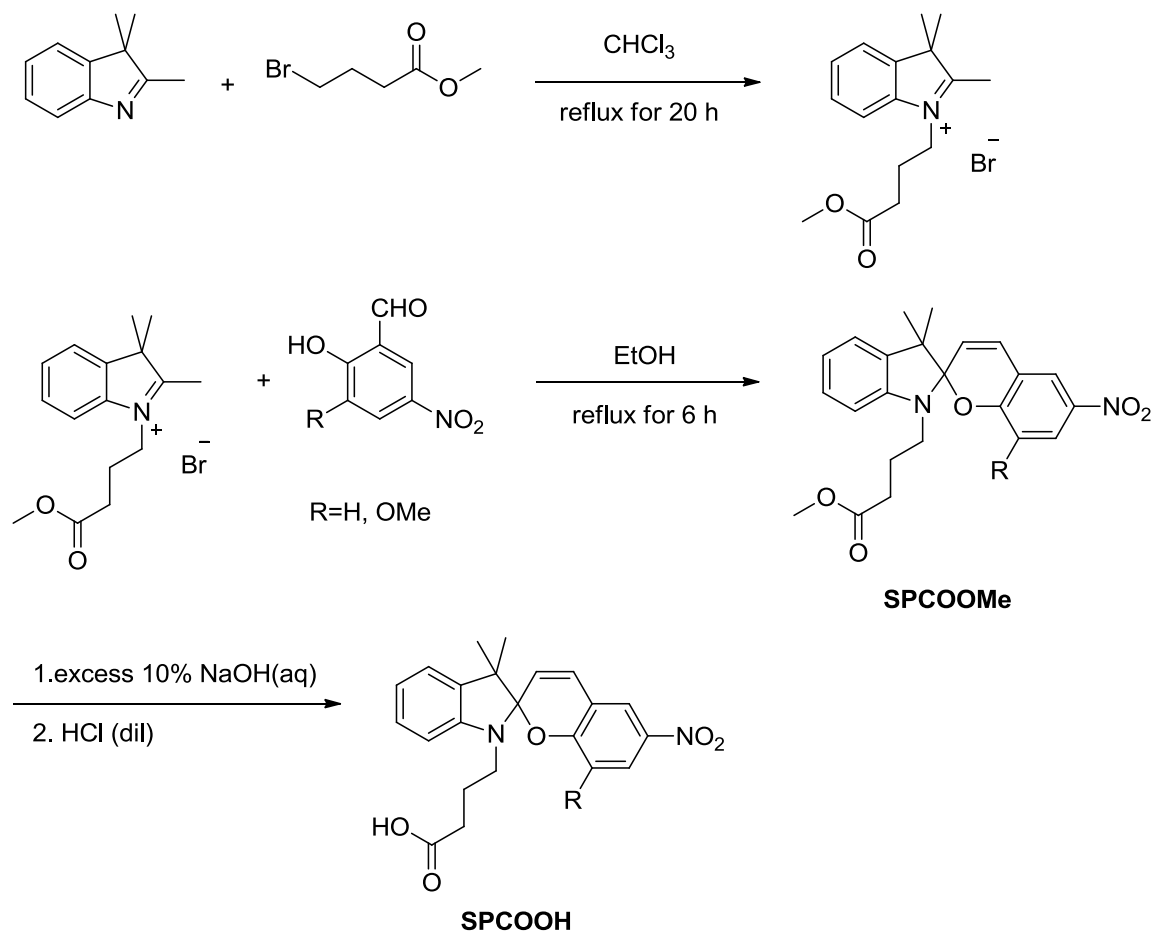
Figure 3.2 Synthesis of spiropyran, with R = H and OCH$_3$.

Synthesis of 1-(3-carbomethoxypropyl)-3,3-dimethyl-2-methyleneindoline

A solution of 2,3,3-trimethylindolenine (8.90 g, 0.0547 mol) and methyl 4-bromobutyrate (9.90 g, 0.0547 mol) in 20 mL of chloroform was refluxed for 20 hours. The solvent was evaporated and the reddish residue was washed with diethyl ether and recrystallized from a mixture of diethyl ether and methanol (9:1) to give 15.50 g (0.0455 mol, 83 %) of the desired indoline as its quaternary ammonium salt.^{1}H NMR (400MHz, MeOD) δ 1.660 (6H, s, CH_3), 2.276 (2H, t, CH$_3$COOCH$_2$CH_2CH$_2$), 2.708 (2H, t, CH$_3$COOCH_2CH$_2$CH$_2$), 3.679 (3H, s, CH_2), 4.621 (2H, t, CH_2N), 7.689 (2H, m, ar-*H*), 7.823 (1H, d, ar-*H*), 8.031 (1H, t, ar-*H*).

Synthesis of 1-(3-carbomethoxypropyl)-3,3-dimethyl-6-nitrospiro{2H-1]-benzo pyran-2,2'-indoline (SPCOOMe)

To 5-nitrosalicylaldehyde (2.6506 g, 0.0134 mol) in 10 mL of ethanol was slowly added to a solution of the quaternary ammonium salt (1-(3-carbomethoxypropyl)-3,3-dimethyl-2-methyleneindoline) (5.0321g, 0.0148 mol) in ethanol. The mixture was refluxed for 6 hours. The resulting dark purple mixture was cooled in an ice bath and filtered. The filter cake was washed with cold ethanol. Three recrystallizations from ethanol gave 2.4530 g (5.594 mol, 42 %). ^{1}H NMR (400MHz, CDCl$_3$) δ1.215 (3H, s, CH_3), 1.310 (3H, s, CH_3), 2.010 (2H, m, COOCH$_3$-CH$_2$-CH_2-CH$_2$-), 2.390 (2H, t, CH_2N), 3.231 (2H, t, CH_2COOCH$_3$), 3.663 (3H, s, COOCH_3), 5.898 (1H, d, *J* = 10.4 Hz, C*H*=CH), 6.669 (1H, d, ar-*H*), 6.771 (1H, d, ar-*H*), 6.923

(1H, t, ar-*H*), 6.928 (1H, d, *J* = 10.4 Hz, CH=C*H*), 7.115 (1H, d, ar-*H*), 7.225 (1H, t, ar-*H*), 8.034 (2H, m, ar-*H*).

Synthesis of 1-(3-carbomethoxypropyl)-3,3-dimethyl-6-nitro-8-methoxyspiro{2H-1]-benzo pyran-2,2'-indoline (SPCOOMe-OMe)

3-Methyoxy-5-nitrosalicylaldehyde (2.6506 g, 13.4 mmol) in 10 mL of ethanol was slowly added to a solution of the quaternary ammonium salt (1-(3-carbomethoxypropyl)-3,3-dimethyl-2-methyleneindoline) (5.0321 g, 14.8 mmol) in ethanol. The mixture was refluxed for 6 hours. The resulting dark purple mixture was cooled in an ice bath and filtered. The filter cake was washed with cold ethanol. Three recrystallizations from ethanol gave 2.4530 g (5.6 mmol, 42 %). ^{1}H NMR (400 MHz, CDCl$_3$) δ 1.201 (3H, s, C*H*$_3$), 1.302 (3H, s, C*H*$_3$), 1.970 (2H, m, COOCH$_3$-CH$_2$- C*H*$_2$-CH$_2$-), 2.375 (2H, t, C*H*$_2$N), 3.274 (2H, t, C*H*$_2$COOCH$_3$), 3.654 (3H, s, COOC*H*$_3$), 3.798 (3H, s, OC*H*$_3$), 5.863 (1H, d, *J*=10.4 Hz, C*H*=CH), 6.648 (1H, d, d, ar-*H*), 6.875 (1H, d, *J*=9.6 Hz, CH=C*H*), 6.896 (1H, t, ar-*H*), 7.097 (1H, d, ar-*H*), 7.203 (1H, t, ar-*H*), 7.647 (1H, s, ar-*H*), 7.713 (1H, s, ar-*H*).

Synthesis of 1'-(3-carboxypropyl)-3',3'-dimethyl-6-nitrospiro[2H-1]-benzopyran-2,2'-indoline (SPCOOH)

1'-(3-Carbomethoxypropyl)-3',3'-dimethyl-6-nitrospiro[2H-1]-benzopyran-2,2'-indoline (1.5693 g, 3.842 mmol) dissolved in 2 mL of tetrahydrofuran was stirred at room temperature for 24 hours with an excess of 10% aqueous sodium hydroxide. The resulting solution was then acidified with dilute hydrochloric acid and was

extracted with chloroform. The chloroform was removed from the organic layer by distillation at reduced pressure, and the residue was chromatographed on silica gel (dichloromethane, containing 10% methanol) to yield 1.4185 g (3.596 mmol, 94 % yield) of the desired spiropyran. ^{1}H NMR (400MHz, CDCl$_3$) δ 1.215 (3H, s, CH_3), 1.310 (3H, s, CH_3), 2.010 (2H, m, COOCH$_3$-CH$_2$-CH_2-CH$_2$), 2.405 (2H, t, CH_2COOCH$_3$), 3.231 (2H, t, CH_2N), 5.898 (1H, d, J = 10.4 Hz, CH=CH), 6.670 (1H, d, ar-H), 6.770 (1H, d, ar-H), 6.919 (1H, t, ar-H), 6.931 (1H, d, J = 10.4 Hz, CH=CH), 7.107 (1H, t, ar-H), 7.222 (1H, t, ar-H), 8.026 (2H, m, ar-H).

Synthesis of 1'-(3-carboxypropyl)-3',3'-dimethyl-6-nitro-8-methoxyspiro[2H-1]-benzopyran-2,2'-indoline (SPCOOH-OMe)

1-(3-carbomethoxypropyl)-3,3-dimethyl-6-nitro-8-methoxyspiro{2H-1]-benzopyran-2,2'-indoline (0.6694 g, 1.5267 mmol) dissolved in 2 mL of tetrahydrofuran was stirred at room temperature for 24 hours with an excess of 10% aqueous sodium hydroxide. The resulting solution was then acidified with dilute hydrochloric acid and was extracted with chloroform. The chloroform was removed from the organic layer by distillation at reduced pressure and the residue was chromatographed on silica gel (dichloromethane, containing 10% methanol) to yield 0.5146 g (1.2123 mmol, 79 % yield) of the desired spiropyran. ^{1}H NMR (400MHz, CDCl$_3$) δ 1.150 (3H, s, CH_3), 1.270 (3H, s, CH_3), 2.010 (2H, m, COOCH$_3$-CH$_2$-CH_2-CH$_2$-), 1.482 (2H, t, CH_2COOCH$_3$), 3.186 (2H, t, CH_2N), 3.763 (3H, s,OCH_3), 5.792 (1H, d, J=10.0 Hz, CH=CH), 6.876 (1H, d, J=8.8 Hz, CH=CH), 6.564 (1H, d, ar-H),

6.669 (1H, d, ar-*H*), 6.893 (1H, t, ar-*H*), 7.101 (1H, t, ar-*H*), 7.617 (1H, s, ar-*H*), 7.687 (1H, s, ar-*H*).

3.3.3. Microfluidic device fabrication

The SU-8 master was fabricated on a silicon wafer via a standard photolithography technique using a maskless exposure system (SF-100, Intelligent Micro Patterning, LLC, St. Petersburg, FL, USA). SU-8 3050 was spun on the wafer at a thickness of ~50 μm according to a recently published program [3]. The wafer was prebaked at 65 and 95 °C, with hold times of 15 and 30 min, respectively. After exposure, the wafer was postbaked with hold times of 5 and 15 min at 65 and 95 °C, respectively. The development was performed using SU-8 developer (Microchem). Finally, the wafer was hard baked at 200 °C to enhance the cross-linking of the developed SU-8. The SU-8 master was then embossed into a PMMA substrate resulting the imprint produced complimentary features in the PMMA substrate. To join PMMA substrates, the temperature-assisted vaporized organic solvent technique was applied for the bonding step. According to work published by Koesdjojo et al.[3], a blank PMMA piece was immersed in chloroform for 1 min to soften the surface of the polymer. The excess solvent left on the surface was allowed to evaporate at room temperature until the surface re-solidified and became firm. Next, the two pieces were pressed together at 400 psi, 65 °C until bonding occurred (Figure 3.3). The PMMA microchip channel dimensions are approximately 2.3 m in length, 100 μm in width, and 50 μm in depth.
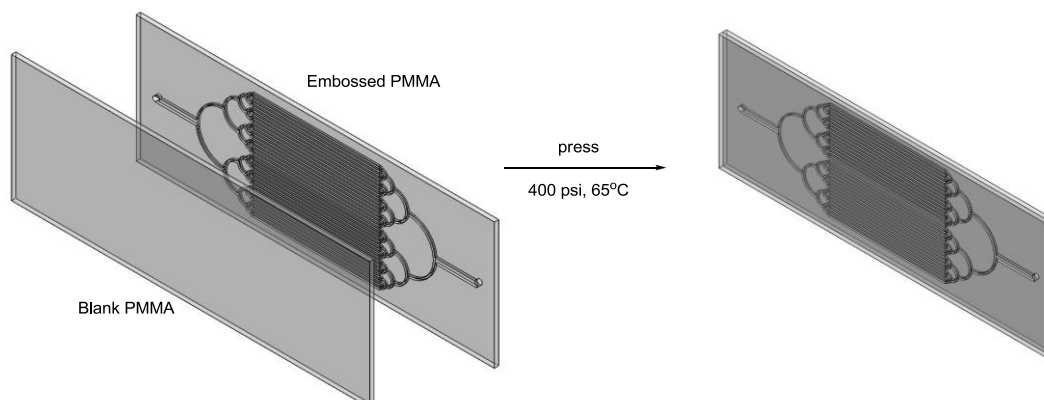
Figure 3.3 Schematic of the microfluidic device. Both the embossed and blank PMMA pieces were surface modified in an oxygen plasma. According to the temperature-assisted vaporized organic solvent bonding technique [3], the two pieces were brought into contact and pressed together at 400 psi, 65 °C until bonding occurred.

3.3.4. Modification of PMMA substrates with spiropyran

Channels on the PMMA microchips were modified in the following manner:

(1). PMMA substrates were sonicated for 10 min in a 50% aqueous 2-propanol solution, and then dried under a stream of nitrogen.

(2). The cleaned PMMA substrate surfaces were activated using a home built oxygen plasma system at 20W and 100mTorr for 5 min [4, 5].

(3). Immediately after plasma modification was completed, the activated PMMA substrates were rinsed with water and 2-propanol, and dried with nitrogen.

(4). The activated PMMA substrates were further modified by immersing them in a 2.5 mg/mL solution of EDC in deionized water for 30 min, followed by the addition of 1,8-diaminooctane (5.5 mg/mL in water).

(5). The PMMA substrates were incubated for 24 hr at room temperature to yield an amine-terminated PMMA surface.

(6). The amine-coated substrates were rinsed with 2-propanol and water to remove unbound diamine groups, and then dried under a stream of nitrogen.

(7). A 75% aqueous ethanol solution containing EDC (2.5 mg/mL) and spiropyran (2.5 mg/mL) was stirred at room temperature for 30 min. The aminated PMMA substrates were then added to this solution and stirred for 36 hr at room temperature. During the incubation period it was important to protect the polymer from light in order to minimize photodegradation of the spiropyran.

The spiropyran modified PMMA substrates were removed and washed with ethanol and water, and then dried under a nitrogen stream.

For lysine bis-spiropyran modified PMMA, the aminated PMMA substrates were immersed in a 5.5 mg/mL solution of the mixture of BOC-lysine (amine protected lysine) and EDC in deionized water for 24 hr at room temperature to yield a BOC-lysine terminated PMMA surface, which was then rinsed with water and 2-

propanol, and dried with nitrogen. The BOC-lysine coated substrates were then deprotected and modified with spiropyrans as described above.

3.3.5. Microfluidic device functionalization

Two oxygen plasma activated PMMA sheets (a blank PMMA sheet and a microchannel-patterned PMMA sheet) were bonded using the solvent-assisted bonding technique as described in 3.3.3 [3]. After fabrication, the microchannels were sequentially filled with the solutions according to the spiropyran surface modification steps using a peristaltic pump at a flow rate of10 µL/min. The pump was connected to the microfluidic device by means of NanoPorts and fittings (Upchurch Scientific, Oak Harbor, WA, USA).

3.3.6. Characterization

Small coupons of PMMA (approximately 1 cm $\times$ 3 cm) were cut and modified according to the spiropyran modification steps listed in 3.3.4. Water contact angle measurements were taken before and after surface modification of the PMMA surfaces using an FTÅ 135 Contact Angle and Video Analysis System (First Ten Angstroms, Portsmouth, VA, USA). 2.0 µL of water was pipetted onto the substrate surface and contact angles were measured in triplicate. The average contact angle for each substrate was reported. In addition, UV-vis spectra of PMMA surfaces before and after surface modification were recorded.

3.3.6. Pb^{2+} extraction set-up

Solutions containing Pb^{2+} were introduced into the microchannels (flow rate 10 µL/min) through each of the inlets by means of a peristaltic pump (ISMATEC 834, Reglo Digital Micropump, Vancouver, WA, USA). The inlets and outlets of the microchannels were connected to the pump by means of NanoPorts and fittings (Upchurch Scientific). Standard aqueous solutions of 50 ppb Pb^{2+} ion were flowed through the channels at 10 µL/min and the Pb^{2+} content before and after irradiation with UV LEDs and green LEDs was quantified using ICP/MS (PQ-EXCELL, Thermo Elemental).

3.4. Results and Discussion

The PMMA microchannel was functionalized with spiropyrans in the following manner. Activation of the PMMA substrate surfaces using oxygen plasma treatment resulted in the introduction of acid groups [5]. The PMMA substrate then was modified with diaminoalkane as a tether. Spiropyran was finally anchored on PMMA surface using EDC coupling agent. Diamond *et al*. have studied the binding characteristic of the dye with metal ions in solution phase and suggested that the metal ion was sandwiched between two merocyanine molecules [5]. However, solution phase chemistry can differ greatly from solid phase chemistry, particularly if the stoichiometry requires convergence of multiple ligands around a single guest species. We were concerned that covalent immobilization of spiropyran molecules to a

polymer surface might inhibit the ability of sandwich complex to form. According to the Diamond studies, using 1,8-diaminooctane as a tether provided sufficient length to enable metal complex [5]. We therefore elected to append spiropyran to microchannels using diaminealkane compound including 1,8-diaminooctane and 1,12-diaminododecane as shown in Figure 3.4a. In addition, spiropyran molecules were needed to allow enough flexibility not only to photoisomorize between the active and passive forms, but also to come together in a sandwich complex with neighboring dye molecule. In order to keep spiropyran molecules close enough to form complex with metal ion, lysine was therefore elected as a spacer between the diamine tether and the dye as shown in Figure 3.4b. The use of bifunctional tethers increases the mol% of SP available and may therefore amplify the achievable extraction efficiency.
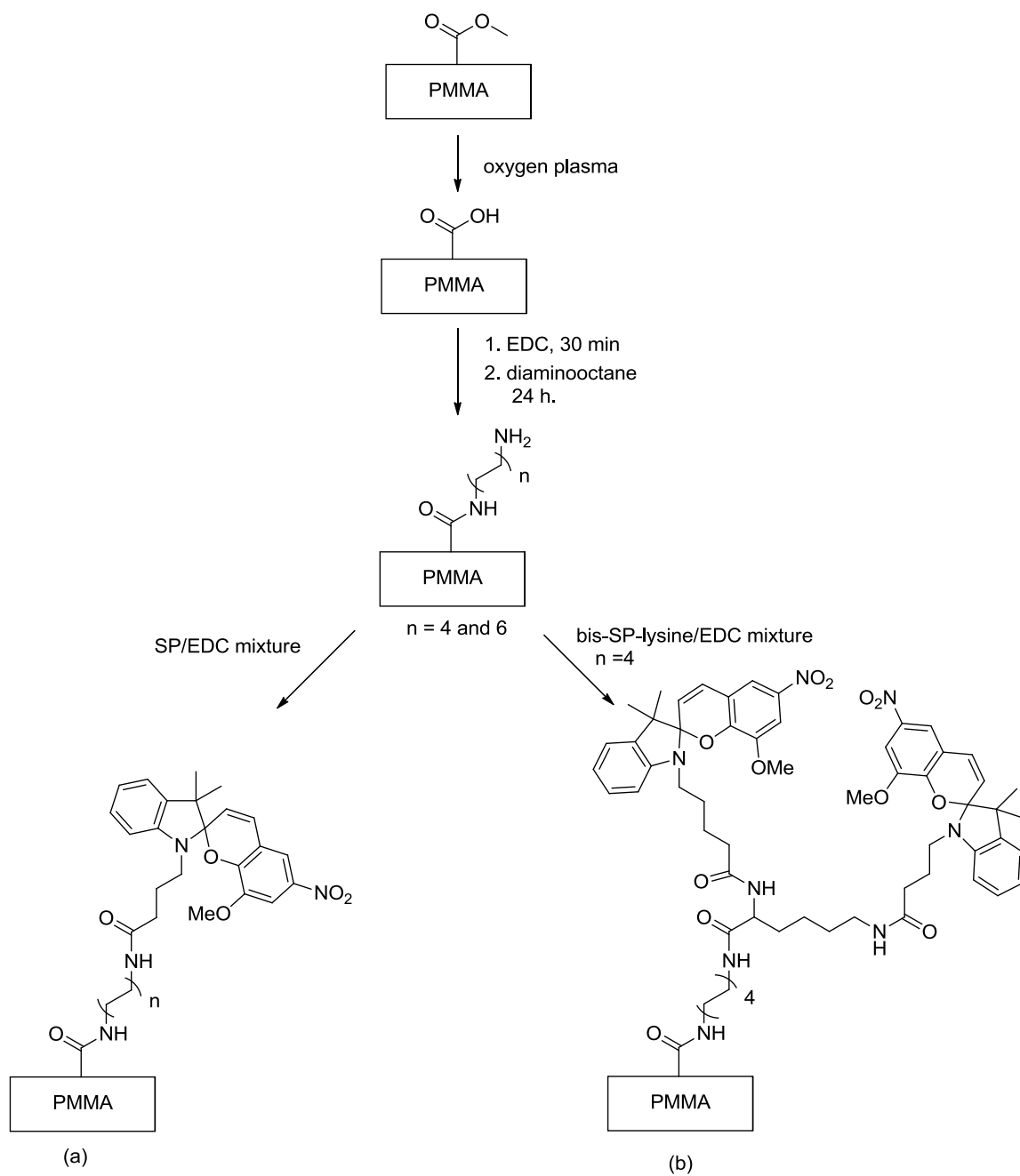
Figure 3.4 Schematic of the tethering of spiropyran (a) and lysine-bis-spiropyran (b) to the PMMA micro-channel surface.

Tethered bis-spiropyran units can be effectively switched between the closed (colorless) and open (purple) forms. Though, to date literature reports on spiropyran switching have involved the use of high power light sources such as mercury arc lamps or lasers. Photo-chemical phase separation has also been induced using nanosecond laser pulse irradiation, and dynamics of the phase domain growth have been studied. Diamond et al. have demonstrated that the use of LEDs instead of more powerful light sources substantially reduced the photobleaching that occurs when switching between the closed and open forms repeatedly over time [6]. In the Diamond work, the LEDs power was only ~1 mW cm^{-2}, whereas, arc lamp light sources are typically 50-100 W cm^{-2}. Despite this large reduction in emissive power, the switching efficiency was relatively unaffected, and repeated switching was successfully performed.

With our bis-spiropyran, irradiation with a UV LED array (390 nm) for 5 min caused the substrates to become purple in color, and the characteristic large absorption band around 590 nm appeared (Figure 3.5). The conversion of MC to the SP form was completely achieved following 15 minutes of irradiation with a green LED array (525 nm). Recall that it was previously confirmed that the green region was the most effective for conversion of MC to the SP form [5].
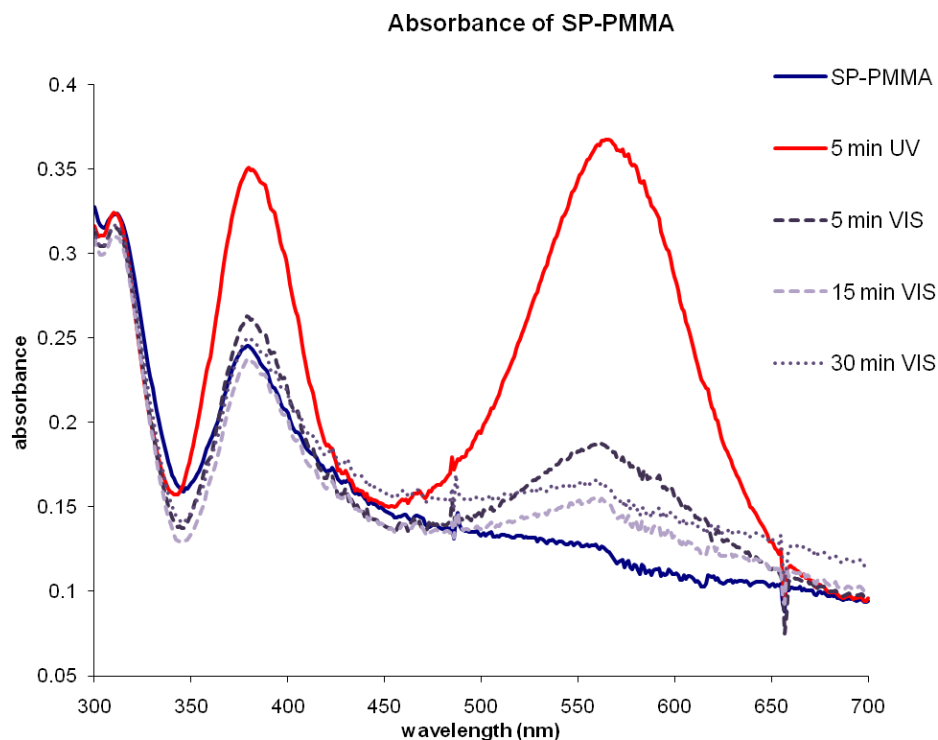
Figure 3.5 Absorption spectrum of a spiropyran, before and after irradiation with 390 nm LED array.

Spiropyrans immobilized on PMMA surfaces likewise demonstrated photoconversion. The photoisomerization cycle was monitored as the change in absorbance of the modified PMMA substrate at 590 nm following irradiation with UV (390 nm, 5 min) or visible light (525 nm, 15 min). As illustrated in Figure 3.6, photoisomerization occurs reversibly, and there is little or no photodegradation of the substrate during the course of several irradiation cycles.
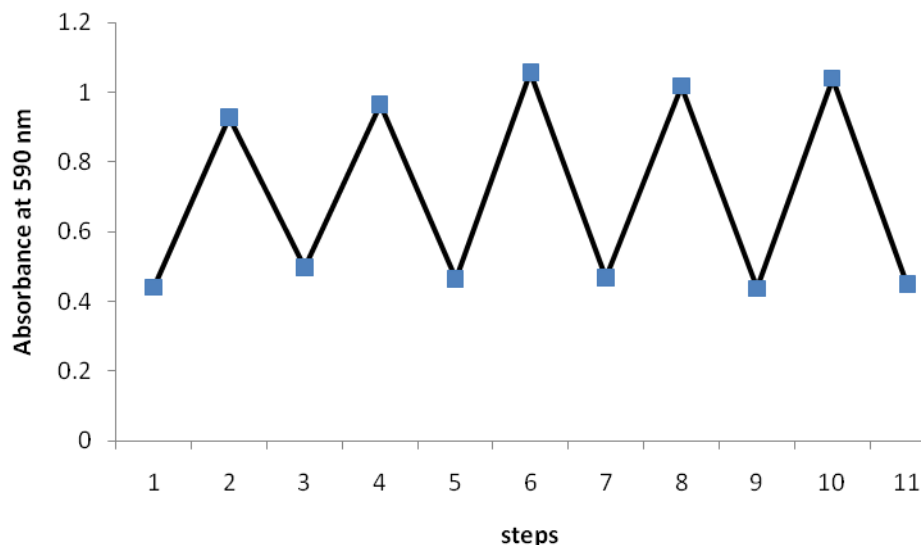
Figure 3.6 Cyclic photoisomerization of spiropyrans immobilized on a PMMA substrate monitored as the absorbance of the closed and open forms at 590 nm.

Here we review some of our findings on reversible, photoinduced wettability changes of polymer surfaces treated with photochromic spiropyran molecules. We illustrate how the hydrophilicity of the surfaces is enhanced upon UV LED irradiation when the embedded non-polar spiropyran molecules convert to their polar merocyanine isomers, and how this process is reversed upon irradiation with green LEDs. Figure 3.7 shows that the contact angle of water on an unmodified PMMA coupon was originally 62.24˚. After SP surface modification and UV irradiation, the contact angle decreased to a value of 32.66˚ as the MC form is significantly more polar and hydrophilic.

(a)	(b)	(c)
PMMA	SP-PMMA	SP-UV
CA =62.24°	CA=69.76°	CA=32.66°
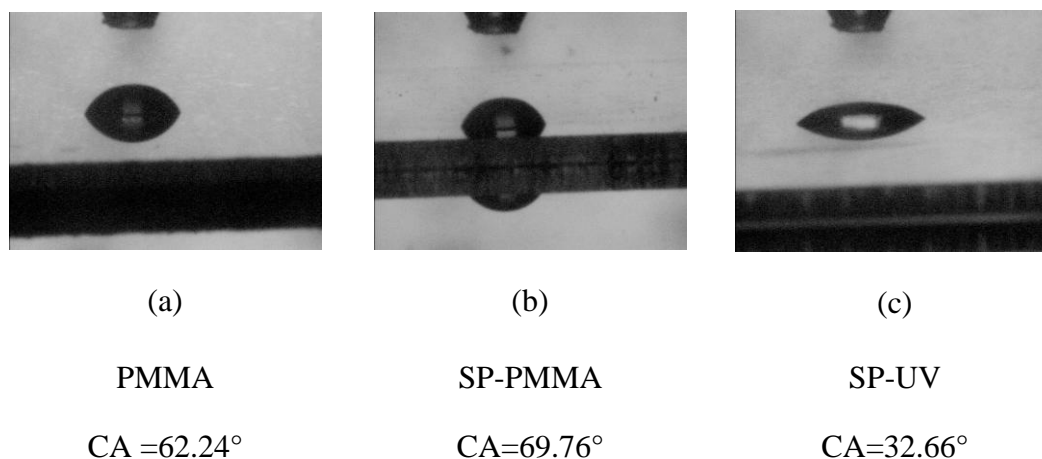
Figure 3.7 Optical microscopy images of the water meniscus on the surface of various native and functionalized PMMA surfaces; (a) untreated PMMA, (b) spiropyran modified PMMA, and (c) spiropyran modified PMMA after 5 min UV irradiation.

When the colorless SP-PMMA is illuminated with UV light (390 nm) the chip channels take on a purple coloration: the color change is easily visualized (Figure 3.8). Thus, the observed color changes upon UV or visible light exposure are indicative of successful modification of surfaces of the PMMA microchannels with spiropyrans, which then are capable of transforming between the SP and MC forms when "gated" with light of the appropriate wavelength.

| (a) | (b) | (c) |
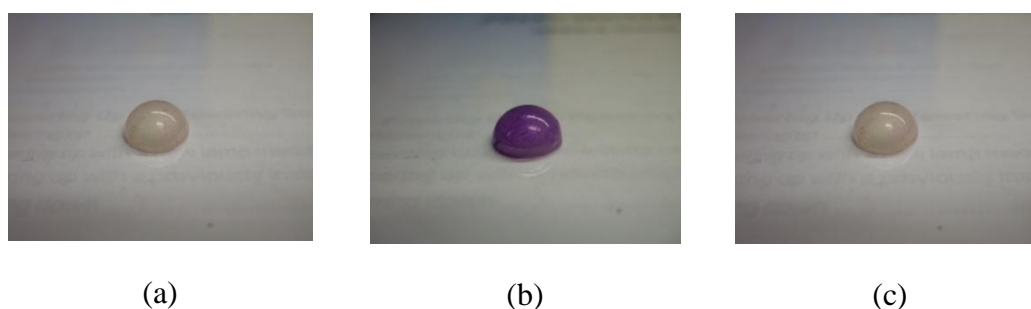
Figure 3.8 Spiropyran-modified PMMA before irradiation with UV light (a), after irradiation with UV light (b), and after irradiation with green light (c).

The PMMA microchip channel dimensions are approximately 2.3 m in length, 100 μm in width, and 50 μm in depth resulting approximately 10 µL in total internal volume. In this work, we have focused only on the spiropyran derivative and its metal binding/releasing properties. Physical coating of the polymer surface with spiropyran intuitively seems to be the simplest solution for its utilization in metal extractions. Unfortunately, the MC form is significantly more polar than the SP form [7] , which makes it prone to leaching from the polymer surface. Covalent attachment of sensing components has emerged as an attractive means to address the problem of insufficient retention of MC [8]. Diamond et al.[5] have demonstrated that modified spiropyran can be attached to the activated PMMA surface with full preservation of the ability of the spiropyran to switch between the active and passive forms. The group utilized the covalently attached spiropyran to detect Co^{2+}. In addition, the switching of spiropyran can be achieved using simple LEDs instead of the conventional light source as a simplification of sensing platform [6]. As shown in Figure 3.9, the photoconversion cycles of spiropyran modified microchannels can be successfully switched with irradiation with UV-vis light.
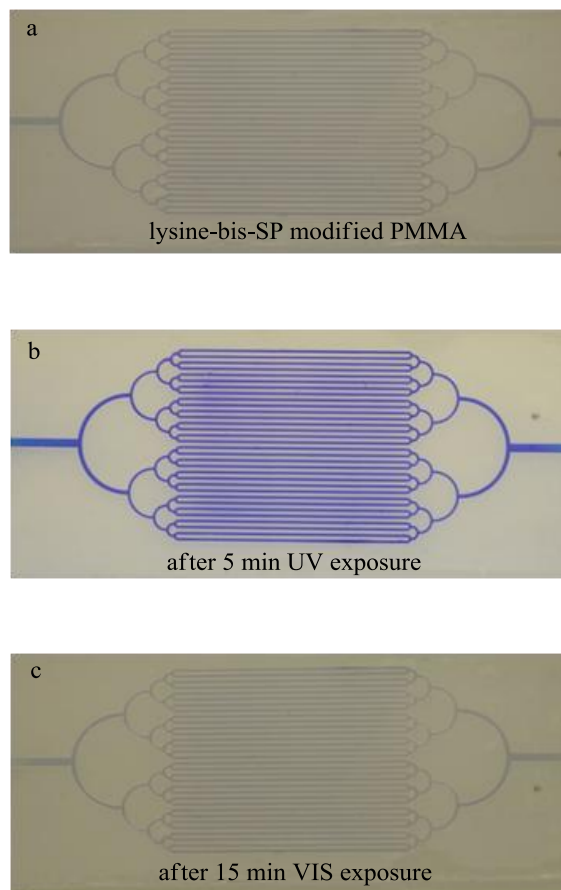
Figure 3.9 the PMMA microchips modified with spiropyran before irradiation with UV light (a), after irradiation with UV light (b), and after irradiation with green light (c).

Initially, spiropyran was present in the SP form and the PMMA microchip appeared transparent. When the PMMA microchip was irradiated with UV light, the SP was converted to MC form, giving rise to a purple coloration. When the microchip in the MC form was exposed to 2 mL of 50 ppb Pb^{2+} aqueous solution with flow rate at 10 μL/min, the binding of Pb^{2+} by the phenolate anion of MC led to the formation of a MC-Pb^{2+} complex. To release the bound Pb^{2+}, the microchip was further irradiated with a green LED array. The Pb^{2+} content from each step was monitored

using ICP/MS. An important consideration in the development of photoswitchable ligands is their binding strength in the activated form. We have studied the intrinsic binding of photochromic molecules to metal ions by producing molecules that contain one-and two-spiropyran units attached to a flexible backbone (Figure 3.10).
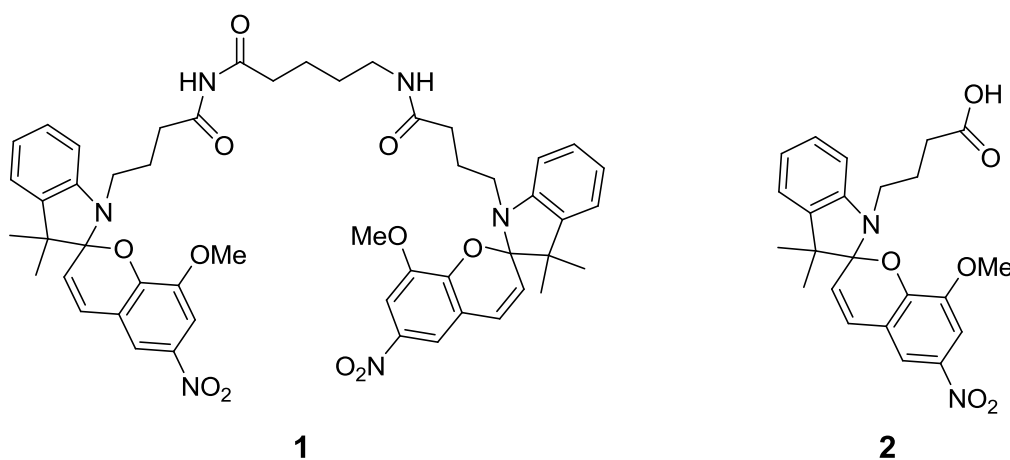
Figure 3.10 Structures of a bis-SP-lysine (1) and SP (2).

Chelation of Pb^{2+} by spiropyran requires two spiropyran molecules per one metal ion. As shown in Figure 3.1, the two phenolic oxygen atoms of the open form can converge on a single metal atom. Spiropyran modified microchannels were used in a series of experiments to determine whether the tether length and addition of lysine as a spacer might influence Pb^{2+} extraction efficiency. It was expected that the formation of the Pb^{2+} complex would be affected by molecular flexibility, and therefore tether length would be important. In addition, lysine which contains two amine groups was used as a spacer to increase the mole percent of spiropyran on the PMMA surfaces.

The efficiency of extraction is essentially determined by two parameters including the percentage of Pb^{2+} extraction and the amount of Pb^{2+} extracted per the

volume of microchannels. The percentage of Pb^{2+} extraction was defined as the percentage of ratio of Pb^{2+} concentration before and after flowed into the microchannels. Table 3.1 shows the effect of tether length and spacer inclusion on the Pb^{2+} extraction efficiency. Clearly, the extraction efficiency improves with lysine as a spacer, as evidenced by increased extraction efficiency for Pb^{2+}. These data suggest that formation of the 2:1 complex would be affect by the spiropyran proximities. Without lysine, the bound spiropyran molecules were insufficiently close to enable metal complexation resulting in lower extraction efficiency. However, there is little change in the extraction efficiency with increasing tether length. These results suggest that a certain minimum distance (approximated by the the 1,8-diaminooctane spacer) is required to facilitate efficient switching to the open form, which involves rearrangement of the molecular structure into a planar, extensively conjugated zwitterion.

Table 3.1 Pb^{2+} Extraction efficiencies measured using spiropyran-modified microfluidic devices. Data from ICP/MS (n = 4)

SP	Percent of Pb^{2+} extraction	mg of Pb^{2+}/L
1.8-diamine-SP	77.03	4.50
1,12-diamine-SP	85.90	5.37
1,8-diamine-lysine-bis-SP	92.38	6.20

3.5. Conclusion

We have successfully demonstrated a novel system enabled via a photoactivable microfluidic device. PMMA microchips decorated with immobilized spiropyrans were successfully used for Pb^{2+} extraction by simply irradiating them with different wavelengths of light. This study showed that spiropyran chelating agents have great potential for the selective sequestration of Pb^{2+}. Advances in the integration of LED sources in the system hold promise for the production of low cost, miniaturized systems. In the present study, the Pb^{2+} content was analyzed off-line; however, by employing another detection method (for example an electrochemical method), on-line monitoring of extraction efficiency is certainly possible.

3.6. Acknowledgement

3.7. References

1.   Winkler, J.D., K. Deshayes, and B. Shao, *Photodynamic transport of metal ions.* Journal of the American Chemical Society, 1989. **111**(2): p. 769-770.

2.   Garcia, A.A., et al., *Photon-controlled phase partitioning of spiropyrans.* Journal of Physical Chemistry A, 2000. **104**(26): p. 6103-6107.

3.   Koesdjojo, M.T., C.R. Koch, and V.T. Remcho, *Technique for Microfabrication of Polymeric-Based Microchips from an SU-8 Master with Temperature-Assisted Vaporized Organic Solvent Bonding.* Analytical Chemistry, 2009. **81**(4): p. 1652-1659.

4.   Brown, L., et al., *Fabrication and characterization of poly(methylmethacrylate) microfluidic devices bonded using surface modifications and solvents.* Lab on a Chip, 2006. **6**(1): p. 66-73.

5.   Byrne, R.J., S.E. Stitzel, and D. Diamond, *Photo-regenerable surface with potential for optical sensing.* Journal of Materials Chemistry, 2006. **16**(14): p. 1332-1337.

6.   Stitzel, S., R. Byrne, and D. Diamond, *LED switching of spiropyran-doped polymer films.* Journal of Materials Science, 2006. **41**(18): p. 5841-5844.

7.   Bletz, M., et al., *Ground- and first-excited-singlet-state electric dipole moments of some photochromic spirobenzopyrans in their spiropyran and merocyanine form.* Journal of Physical Chemistry A, 2002. **106**(10): p. 2232-2236.

8.   Bakker, E. and Y. Qin, *Electrochemical Sensors.* Analytical Chemistry, 2006. **78**(12): p. 3965-3984.

CHAPTER 4

FABRICATION OF HYBRID GLASS POLY(TETRAFLUOROETHYLENE)
MICROFLUIDIC DEVICE

Jintana Nammoonnoy, Taehyeong Kim, Jeffrey R. Walker, and Vincent T. Remcho

Department of Chemistry, Oregon State University, Corvallis, OR 97331

4.1. Abstract

The work demonstrates a new fabrication technique based on a chemically activated poly(tetrafluoroethylene) (PTFE) sheet sandwiched between chemically activated glass substrates. PTFE microchannels were fabricated using a cutting plotter which can consistently achieve microchannels as narrow as 200 μm in minutes, and can be used to fabricate an extremely robust microfluidic device without the need of harsh chemical etchants. To facilitate this, the surface of glass substrate is functionalized with aminopropyl triethoxysilane (APTES) which contains terminal amine groups, while the PTFE surface is activated to form carboxylic groups and subsequently coupled with 1-ethyl-3-[3-dimethylaminopropyl]-carbodiimide hydrochloride/N-hydroxy sulfo succinimide sodium salt (EDC-NHS) coupling agents. Robust bonds are created at elevated temperature (150 °C) by simply pressing two amine-terminated glass substrates together with an activated PTFE sheet sandwiched in between.

4.2. Introduction

Chip-based microfluidic devices have attracted broad interest in recent years as researchers have explored as μTAS systems [1-4]. Although microfluidic devices may be produced from glass, quartz, silicon, and various polymeric materials, glass substrates have been employed most frequently because of their well established fabrication procedures and many beneficial characteristics, such as their optical properties, high voltage tolerance, chemical resistivity, high thermal stability and biocompatibility [2-4]. In spite of their advantages, glass microchips also have some limitations, namely their high unit cost and specialized fabrication procedures.

More recently, plastics have become popular as structural materials for microfluidic devices due to their reduced fabrication cost opening the door to single-use or disposable devices [5]. Microfluidic devices are most often fabricated by creating open microfluidic channels on flat substrates and then encapsulating or sealing the channels with a flat polymeric or inorganic sheet or film. Several methods have been demonstrated that bond the polymer layers used in building microfluidic devices , for example, thermal bonding [6], lamination [7], adhesives [8], solvent welding, and surface activation [9, 10]. In thermal bonding, interlayer adhesion is achieved by heating the substrate near its glass transition temperature while applying pressure normal to the surface, allowing the polymer chains to diffuse between the mating surfaces for high bond strength. While effective, thermal bonding presents several disadvantages. Since the substrates must be heated to or slightly above their glass transition temperatures, microchannels may be deformed or collapsed during the bonding process. This is especially problematic for low-aspect-ratio channels and thin substrates. This is termed "dimensional instability". Moreover, the resulting bond strength is often lower than desired, limiting the application of devices produced in this manner to low pressure techniques. Solvent bonding can also suffer from dimensional instability, since the absorbed solvent softens the polymer to enable bonding, and therefore may also and eventually collapse channels. To minimize these problems in PMMA microfluidic chips, carefully controlled, highly specific solvent conditions [6, 11, 12] or sacrificial materials [13] have been employed. For solvent assisted bonding, optimization is required for each different polymer grade and type.

Furthermore, solvents may embrittle thermoplastics, that result in microcracking; this is particularly problematic for microfluidic systems intended for use with high pressure loading. Alternatively, adhesive bonding may be applied in microfluidic fabrication. The primary disadvantage of using adhesives is that they may flow into the channels and block the flow. For these reasons, surface modification-assisted bonding methods have been demonstrated [10, 14, 15]. In general, these methods facilitate bonding through a chemical reaction that occurs selectively at the interface between two solid materials. Because of these challenges, there remains a need for effective methods for microfluidic fabrication.

Recently, a room-temperature bonding technique based on chemically activated fluorinated ethylene propylene (FEP) sheet as an intermediate between chemically activated substrates was reported by Bart et al. [16]. The surfaces of the FEP sheets were treated with a Fluoroetch® solution to generate a carboxylated surface that is subsequently converted to an amine-reactive sulfo-NHS ester, while the surfaces of glass slides were modified with APTES. Etched microchip structures were fabricated from borosilicate glass substrates by standard photolithography and wet chemical etching techniques: an effective but tedious and expensive method.

To overcome these limitations, we have explored the possibility of fabricating extremely robust microfluidic devices entirely from fluorocarbon and glass materials. The use of PTFE is motivated by its well-established chemical inertness and durability over extremes of temperature. PTFE microchannels can be fabricated in minutes using

a cutting plotter to create microchannels. Our method for bonding glass and to PTFE makes possible a wide range of applications.

4.3. Experimental

4.3.1. Device Fabrication

Devices were fabricated in three-layer stacks, comprised of a upper glass layer, a PTFE center (channel) layer, and a lower glass layer (Figure 4.1) Inlets and outlets were drilled using a laser drill (ESI 5330, Electro Scientific Industries, Inc., Portland, OR USA). The PTFE layer was fabricated using a cutting plotter (Cutting Pro FC2250-60, Graphtec America Inc. Santa Ana, CA, USA).

Upper Glass Layer

PTFE Channel Spacer

lower Glass Layer
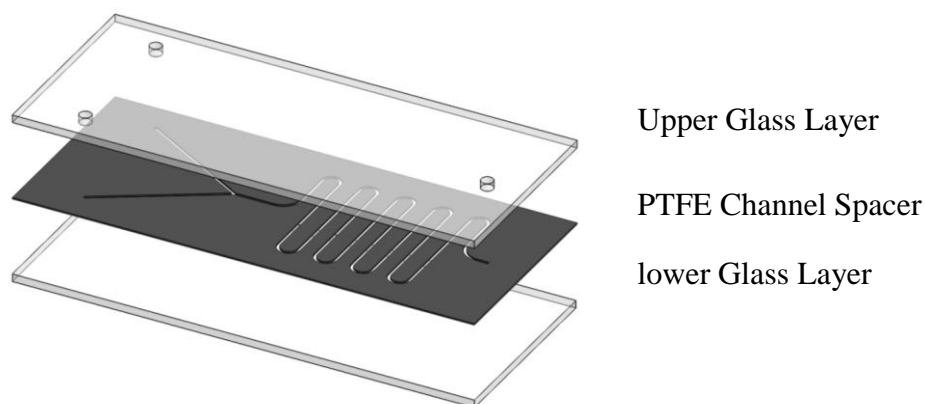
Figure 4.1 Fabrication of glass-PTFE microfluidic device. The channels are cut on an activated PTFE sheet using a cutting plotter. The PTFE channels are sandwiched between two glass slides for bonding.

4.3.2. Preparation of glass substrates

Prior to coupling the amine-terminated activation layer, the glass substrates were painstakingly cleaned. Borosilicate glass substrates (Fisherbrand® glass

microscope slides, precleaned, 25×75 mm, thickness 1 mm, , Fisher Scientific, USA) were ultrasonically cleaned by immersion in isopropanol (15 min; technical grade). In order to further clean and activate the surfaces, the slides were immersed in boiling piranha solution for 30 min (3:1 v/v mixture of 98% sulfuric acid (EMD Chemical, USA) and 31% aqueous hydrogen peroxide (Mallinckrodt Chemical, USA), rapidly rinsed in deionized water, and dried under nitrogen flow. An aminopropyltriethoxysilane solution, having concentration 5% v/v of (APTES, Sigma Aldrich, WI, USA) in acetone, adjusted pH to 4.5-5.5 with acetic acid, was prepared in an airtight glass bottle. Hydrolysis was allowed to occur for 5 min at room temperature to generate reactive silanols, and the slides were then incubated in the APTES solution at 120 °C for 30 min before being removed from the solution and washed well in acetone to remove excess reagent. The slides were then cured in an oven at 120 °C for 1h.

4.3.3. PTFE sheet treatment

Since a carboxylated surface was needed for the EDC-NHS coupling chemistry, it was necessary to strip fluorine from the polymer backbone. An etching solution containing sodium naphthalene was used for this purpose. Sodium strips the fluorine from the carbon backbone and promotes its replacement with hydroxyl, carbonyl and carboxyl groups; under the conditions we employed this result in a PTFE sheet of which the surface is rich in carboxylic groups (Figure 4.2). The fluorine stripping process affects only the surface of the sheet (less than a nanometer of penetration), and the bulk of the polymer remains unaffected [16]. Since each step of

the activation process relied on success in the previous step, it was necessary to characterize the surface chemistry of the PTFE film at each step in the pathway via contact angle measurements.
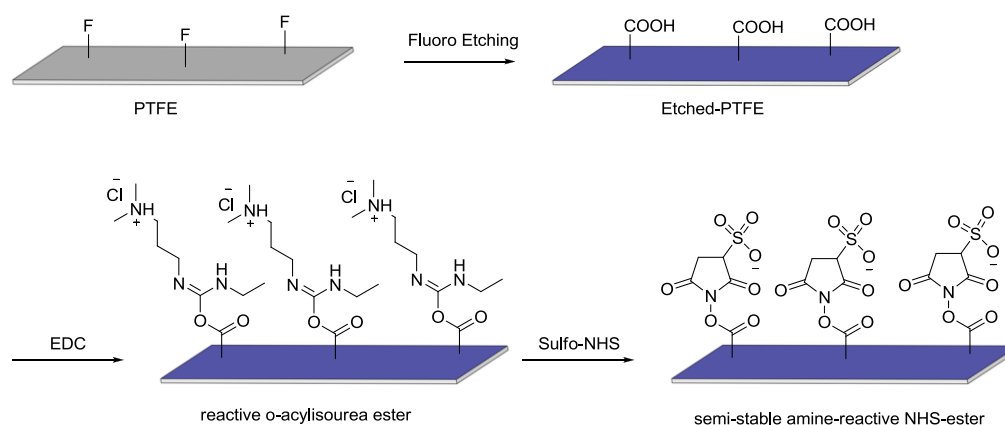
Figure 4.2 Schematic of activation of the PTFE substrate.

The etched-PTFE sheet (thickness 127 μm, Professional Plastics, Fullerton CA, USA) has a brownish color, due to the presence of sodium naphthalene residues. According to Bart's work, it was found the piranha solution effectively removes these residues; however, it also attacks the fluorine-free top layer [16]. The etched-PTFE sheets were immersed in the piranha solution at 60 °C for 2 min. After removal of the residues the sheets were extensively flushed with de-ionized water, and dried with a nitrogen stream. The EDC-NHS solution was prepared as follows: 20 mM of N-hydroxy sulfo succinimide sodium salt (sulfo-NHS; Thermo Scientific) and 50 mM of 1-ethyl-3-[3-dimethylaminopropyl]-carbodiimide hydrochloride (EDC, Sigma Aldrich, WI, USA) were dissolved in de-ionized water. The mixture was allowed to

mix for 15 min prior to immersion of the PTFE sheets. Cleaned, etched PTFE coupons (25.4 ×76.2 mm) were immersed horizontally in the EDC-NHS mixture. After 1 hour of incubation at room temperature, the coupons were then inverted and incubated for another hour, the goal being to achieve a homogeneous coverage on both sides of the coupon. Finally, the coupons were rinsed with de-ionized water and dried under a nitrogen stream.

4.3.4. Bonding procedure

After APTES functionalization, the glass slides and EDC-NHS activation of the PTFE coupons, "stacks" comprising a glass slide, PTFE coupon, and a glass slide were prepared. On a support substrate (6" diameter silicon wafer), glass slides were positioned with their amine-terminated side upwards. On these samples NHS-modified PTFE coupons were positioned, and were covered with glass slides in such a way that the amine-terminated side faced the NHS-modified PTFE (Figure 4.3).
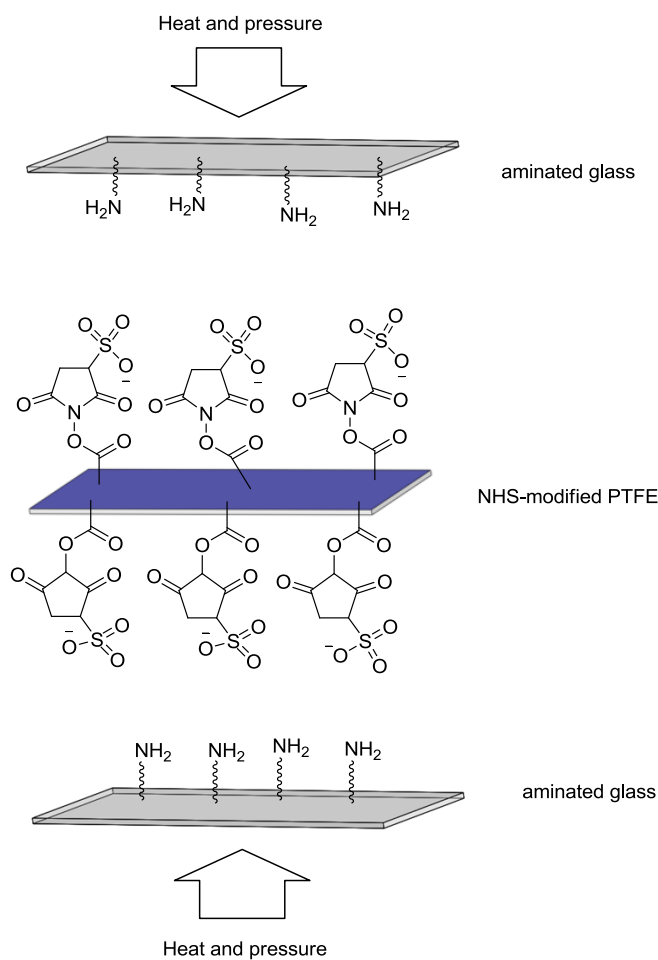
Figure 4.3 The stacks comprising of a upper aminated glass slide, a center NHS-modified PTFE coupon and a lower aminated glass slide for bonding process.

In order to ensure a uniform force distribution on all stacks during compressing, a PDMS layer was used as a support/substrate. After alignment of the samples the stacks were manually compressed using a hydraulic press (Carver Inc., Model 3851-0) at 400 psi for 4 h at 150°C (In this procedure, the load was applied after the system had been heated to the desired temperature.)

4.3.5. Characterization

Water contact angle measurements were taken before and after surface modification of the glass slides and PTFE sheets using a FTÅ 135 contact angle and video analysis system (First Ten Angstroms, Portsmouth, VA, USA). 3.0 µL of water was pipetted onto the substrate surface, and contact angles were measured in triplicate and the average contact angle for each substrate was reported.

4.4. Results and discussion

The glass slides and PTFE coupons were characterized before and after modification by means of contact angle measurement. The contact angle of the cleaned glass slides (10.28°) increased after the amine immobilization process (39.94°) as would be expected. The contact angle measured on APTES-treated glass slides agreed with the data reported in the literature [17] and confirmed the proper immobilization of an amine-terminated self-assembled monolayer (SAM) on the surface (Figure 4.4).
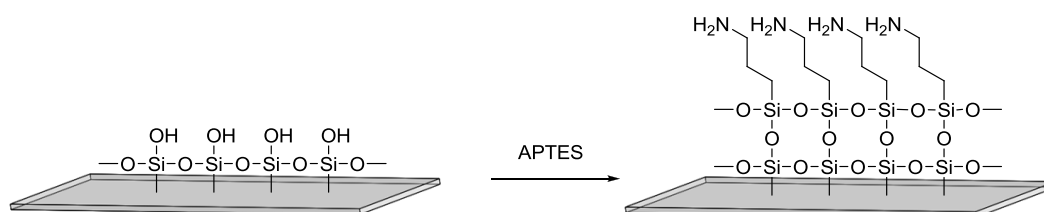
Figure 4.4 Schematic of an APTES functionalized on glass coupon.

The brownish color of the PTFE coupon indicated the presence of a sodium naphthalene residue on the surface, thus the coupon was etched prior to use. A contact angle of 31.04° was observed for the etched-PTFE sheet. It has been reported that the contact angle for carboxylate-terminated surface is typically below 25°, depending on the surface smoothness and layer-density [18]. We suspect that the etching process is not exhaustive, and that these remain a small amount of sodium naphthalene on the surface. In Bart's work, it was found that piranha solution effectively removed these residues when the temperature and etch time in piranha solution were optimized [16]. Measurement of the contact angle on the PTFE surface after more through residual layer removal suggested a further reduction of the residue layer (Figure 4.5). The contact angle after 2 min of piranha cleaning fell below 10°, which suggested the desired carboxylic acid-rich surface. In addition, following EDC-NHS immobilization, a contact angle of 20.81° was measured.

PTFE	Etched-PTFE
106.37±2.47°	31.04±2.76°
2 min Piranha	EDC-NHS immob.
5.15±0.57°	20.81±0.95°
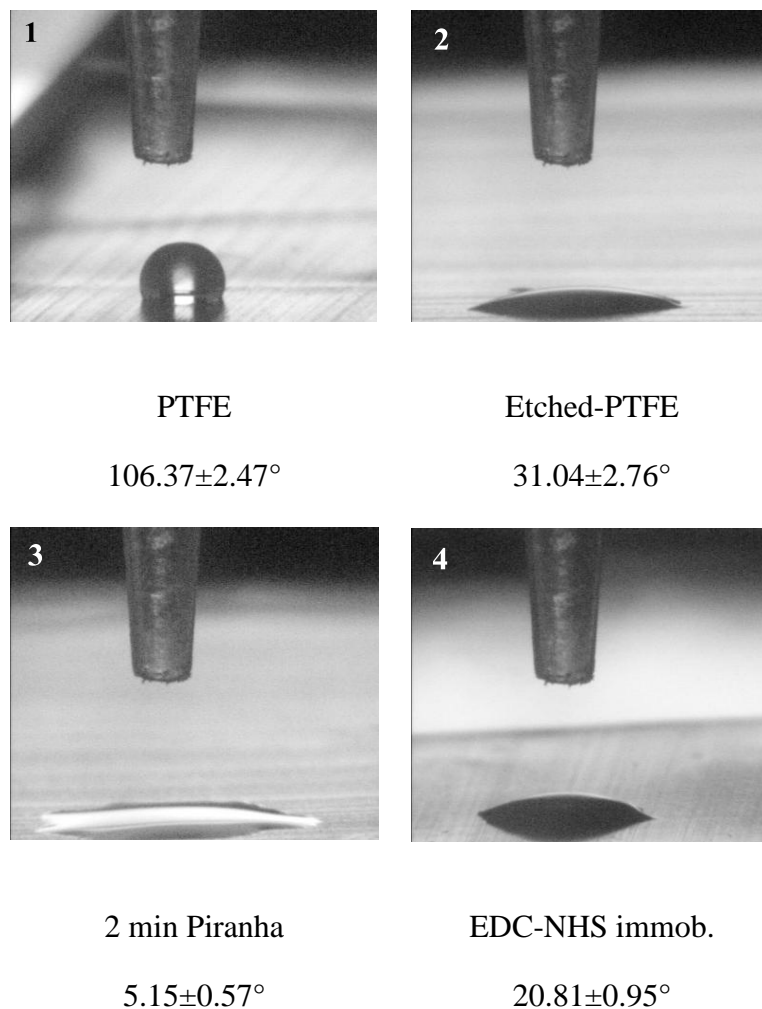
Figure 4.5 Representative contact angle results obtained before and after successive steps in the EDC-NHS activation of aPTFE sheet.

Rather than forming the microchannel on the glass substrate using a standard photolithography and wet chemical etching technique, the channel was created in the PTFE layer using a cutting plotter. This approach allows for rapid chip design and manufacture. The resolution of the cutting plotter depends on the sharpness of the cutting blade, blade adjustment, cutting media, cutting speed, material thickness, and condition of the cutting mat. In order to further investigate the utility of the cutting

plotter for microfluidic device fabrication using activated PTFE sheet, the microchannels with widths ranging from 50 µm to 400 µm were designed and cut (Figure 4.6). Since the plotter is not designed for creating of intricate microfluidic devices, it was more difficult to achieve a clean good-quality cut for narrow (50 µm) microchannels in the PTFE sheeting used in this study.
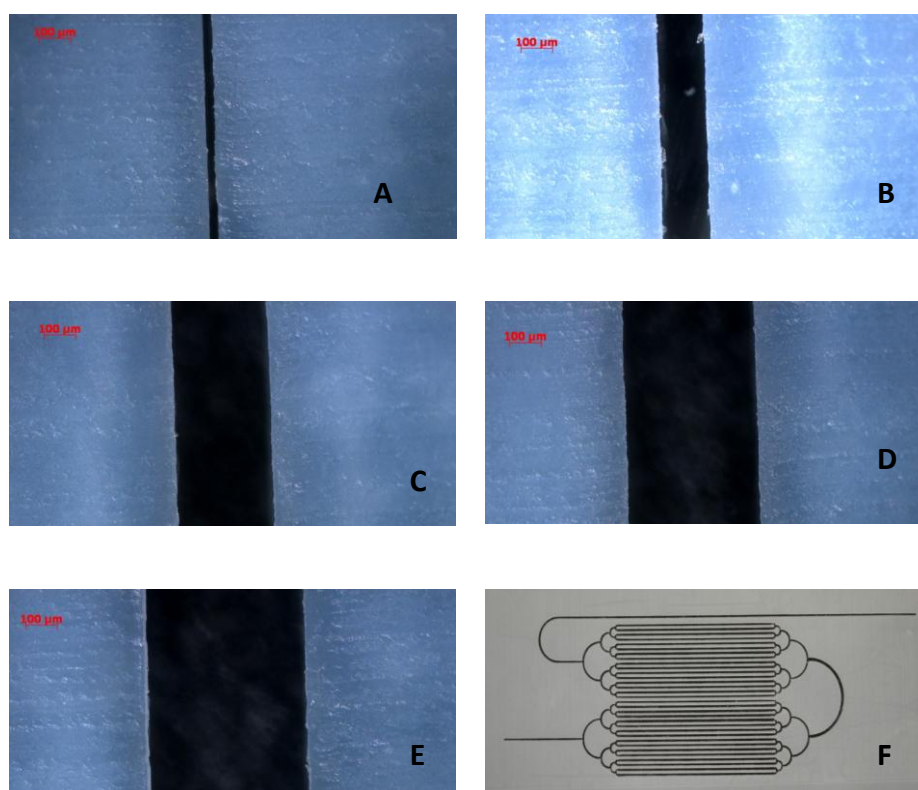
Figure 4.6 Microscopic images of microchannels of 50 µm (A), 100 µm (B), 200 µm (C), 300 µm (D), and 400 µm (E) width with channel depth of 127 µm (the PTFE sheet thickness). (F) A microchannel image shows the cutting quality with a more complex design on the PTFE sheet.

One of the most important factors affecting successful bonding of hybrid-PFTE-glass chips is the cleanliness of the bonding surface of the glass substrate. It has been shown that most unsuccessful bonding events are attributable to the presence of

solid particles or organic material on the glass surface (for example, dust particles, and grease, etc) prior to bonding. Another factor affecting the bond strength is the surface smoothness of the PTFE sheet. Commercial PTFE sheet goods are typically produced by "skiving", a process in which thin sheets of PTFE are mechanically cut from a large, solid spool. However, on the microscale, this cutting process introduces scratches and grooves into the material. These features reduce the amount of surface area available for interaction at glass interfaces in microfluidic devices, making bonding problematic. Therefore, heat (150°C) was applied during our bonding process to soften the PTFE sheet and increase the contact area between the glass substrate and the PTFE surface. With application of heat during the bonding process, the desired thickness of PTFE was preserved as shown in Figure 4.7C.
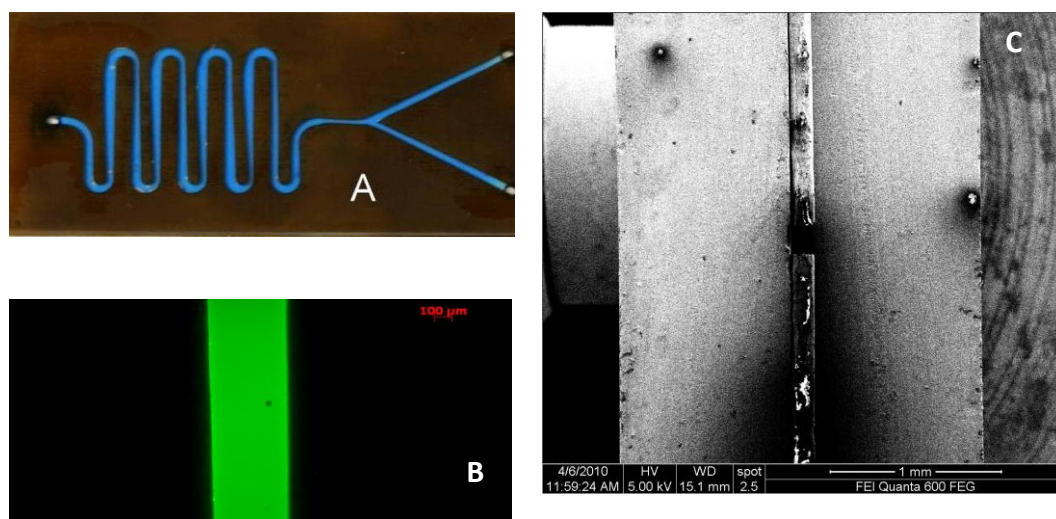
Figure 4.7 Images of a glass/PTFE/glass microfluidic device. (A) Bond integrity test with bromophenol blue indicates no leaks. (B) Fluorescence microscopy image of another bonding test with Rhodamine B solution shows no leaks along the side of microchannel. (C) Scanning electron microscope image of a hybrid PTFE-glass device cross section.

4.5. Conclusion

Effective bonding of PTFE-glass microfluidic devices has been achieved, and is demonstrably simpler and more direct than the tedious and expensive methods by which glass microchannel systems are currently fabricated. The channel is simply formed by cutting the PTFE sheet using a cutting plotter. The hybrid glass-PTFE microfluidic devices can be fabricated using chemically activated PTFE sheets as spacers between chemically activated glass substrates. The glass surface is first functionalized with an amine, while the PTFE sheet surface is treated to yield carboxyl groups and further activated with an EDC-NHS coupling agent. The surface-modified substrates were characterized by means of contact angle measurement. Bonding was successfully realized by simply pressing the two APTES-modified glass substrates together around an EDC-NHS activated-PTFE sheet.

4.6. Acknowledgements

4.7. References

1.   Becker, H. and C. Gärtner, *Polymer microfabrication technologies for microfluidic systems.* Analytical and Bioanalytical Chemistry, 2008. **390**(1): p. 89-111.

2.   Manz, A., et al., *Micromachining of monocrystalline silicon and glass for chemical analysis systems A look into next century's technology or just a fashionable craze?* TrAC Trends in Analytical Chemistry, 1991. **10**(5): p. 144-149.

3.   Jacobson, S.C., et al., *Effects of Injection Schemes and Column Geometry on the Performance of Microchip Electrophoresis Devices.* Analytical Chemistry, 1994. **66**(7): p. 1107-1113.

4.   Harrison, D.J., et al., *Capillary electrophoresis and sample injection systems integrated on a planar glass chip.* Analytical Chemistry, 1992. **64**(17): p. 1926-1932.

5.   Boone, T., et al., *Plastic advances microfluidic devices.* Analytical Chemistry, 2002. **74**(3): p. 78A-86A.

6.   Sun, Y., Y.C. Kwok, and N.T. Nguyen, *Low-pressure, high-temperature thermal bonding of polymeric microfluidic devices and their applications for electrophoretic separation.* Journal of Micromechanics and Microengineering, 2006. **16**(8): p. 1681-1688.

7.   Rossier, J., F. Reymond, and P.E. Michel, *Polymer microfluidic chips for electrochemical and biochemical analyses.* Electrophoresis, 2002. **23**(6): p. 858-867.

8.   Blanco, F.J., et al., *Novel three-dimensional embedded SU-8 microchannels fabricated using a low temperature full wafer adhesive bonding.* Journal of Micromechanics and Microengineering, 2004. **14**(7): p. 1047-1056.

9.   Duffy, D.C., et al., *Rapid prototyping of microfluidic systems in poly(dimethylsiloxane).* Analytical Chemistry, 1998. **70**(23): p. 4974-4984.

10.   Tennico, Y.H., et al., *Surface modification-assisted bonding of polymer-based microfluidic devices.* Sensors and Actuators B: Chemical, 2010. **143**(2): p. 799-804.

11.   Brown, L., et al., *Fabrication and characterization of poly(methylmethacrylate) microfluidic devices bonded using surface modifications and solvents.* Lab on a Chip, 2006. **6**(1): p. 66-73.

12.   Kelly, R.T. and A.T. Woolley, *Thermal Bonding of Polymeric Capillary Electrophoresis Microdevices in Water.* Analytical Chemistry, 2003. **75**(8): p. 1941-1945.

13.   Koesdjojo, M.T., Y.H. Tennico, and V.T. Reincho, *Fabrication of a microfluidic system for capillary electrophoresis using a two-stage embossing*

technique and solvent welding on poly(methyl methacrylate) with water as a sacrificial layer. Analytical Chemistry, 2008. **80**(7): p. 2311-2318.

14. Tsao, C.W., et al., *Low temperature bonding of PMMA and COC microfluidic substrates using UV/ozone surface treatment.* Lab on a Chip, 2007. **7**(4): p. 499-505.

15. Vlachopoulou, M.E. and et al., *A low temperature surface modification assisted method for bonding plastic substrates.* Journal of Micromechanics and Microengineering, 2009. **19**(1): p. 015007.

16. Bart, J., et al., *Room-temperature intermediate layer bonding for microfluidic devices.* Lab on a Chip, 2009. **9**(24): p. 3481-3488.

17. Balachander, N. and C.N. Sukenik, *Monolayer transformation by nucleophilic substitution: Applications to the creation of new monolayer assemblies.* Langmuir, 1990. **6**(11): p. 1621-1627.

18. Lee, T.R., et al., *The Wetting of Monolayer Films Exposing Ionizable Acids and Bases.* Langmuir, 1994. **10**(3): p. 741-749.

CHAPTER 5

SUMMARY AND CONCLUSIONS

The removal of heavy metal ions is a key component in the purification of ground, lake and river water for the purpose of providing water for human consumption, in industrial and agricultural applications, and for the environment. Although ion-exchange resins currently play a significant role in such purifications, they still present a challenge that requires the use of ancillary reagents on a stoichiometric basis in the removal process. For example they are employed to transform the chelating moiety into its "binding" form prior to the introduction of the contaminated sample. Once the complex is formed, other reagents must be introduced to induce rapid conversion to the "non-binding" form and trigger the release of the heavy metal ions. The high consumption of these reagents results in an increase in the waste stream volume and constitutes a high recurring cost that must be borne by the user.

The main objective of this dissertation was to provide a means for the removal of heavy metal ions from an aqueous solution without the use of ancillary reagent to alternate between the two chelating moiety forms. As an alternative, light was used to trigger these events: UV light for setting to the "binding" form and visible light to prompt its conversion into the "non-binding" form. My research focused, in part, on anchoring a novel photochelator onto a solid support.

Photochromism (a reversible change in optical absorbances induced by irradiation with different wavelengths of light) often occurs by photoisomerization of a dissolved organic compound. Among photochromic molecules, spiropyrans, which are comprised of a group of light-switching organic moieties, allow reversible switching between a colorless closed form and an intensely colored merocyanine open form. The photochromism of spiropyrans involves a conversion between two states caused by photo-cleavage of the spiro C-O bond. When the colorless and inactive spiropyran absorbs UV light, it switches into the colored merocyanine form, which also has an active binding site for certain metal ions. Therefore, metal ion uptake can be triggered upon UV irradiation and subsequently reversed on demand by shining green light on the colored complex to regenerate the inactive spiropyran form, resulting in the release of metal ions.

In this dissertation, I developed a novel device that harnesses the unique properties of spiropyrans in a microfluidic platform to achieve large volume water reclamation with minimal waste generation and power requirement. Key components of this dissertation include: the synthesis and characterization of spiropyran derivatives, preparation and characterization of spiropyrans grafted to solid supports, the utilization of these sorbents for Pb^{2+} extraction, and finally the incorporation of the solid support in a microfluidic device for large volume water purification.

To facilitate metal ion chelation, an electron withdrawing substituent group was needed in order to obtain a stabilized, open form spiropyran. The addition of an

electron donor group on a pyran moiety was undertaken to generate an auxiliary ligating group capable of forming a complex with the metal ions. In order to tailor spiropyran structures for use in metal ion extraction, I have synthesized spiropyran derivatives by the straightforward coupling of indoleninium salts and salicylaldehyde derivatives and studied the effects of the substituent groups on the stability of the open form spiropyran. It was clearly indicated that the stability of the dye after exposure to UV light dramatically improved with the addition of a nitro group at the 6-position on the oxybenzene ring, as evidenced by an increase in the open form spiropyran life-time in acetone. In order to introduce the electron donor group, I designed spiropyran derivatives that incorporated a methoxy moiety at the 8-position, in which cation-binding is enhanced upon photoisomerization to their corresponding merocyanine form.

As stated in chapter 2, I successfully utilized spiropyran-modified resins for photoreversible Pb^{2+} extraction. A novel immobilization strategy was necessary to provide sufficient flexibility in the ligating moiety for the spiropyran molecules to come together in a sandwich complex with neighboring dye molecules. Therefore, 1,8-diaminooctane was used as a linker. Further, increase in Pb^{2+} loading capacity was observed with an electron donor group on the spiropyran ring. Even though, spiropyran-modified resins provided high extraction efficiency, there is a limitation as increasing amount of resins, resulting in the insufficient of light penetration through a packed bed resin. Moreover, as functional groups located randomly on the resin surfaces there was a challenging to keep spiropyran molecules in close proximity to

form complex with metal ion. The platform with flat, high transparency and providing high surface per volume ratio was expected to allow more favorable breakthrough performance compared to spiropyran-modified resins evaluated.

To address the issue described above, in chapter 3 we presented a continuous Pb^{2+} extraction on spiropyran-modified microfluidic chips. The PMMA microchips were fabricated using hot embossing and solvent bonding techniques. This study showed that the use of a spiropyran as a chelating agent for Pb^{2+} binding/release processes was effective. Advances in the integration of LED sources in the system hold promise for the production of low cost miniaturized systems.

A major challenge in working with PMMA microchips is that the channel may collapse during surface modification or chip bonding due to exposure to organic solvents. Such limitations led us to explore other fabrication techniques and materials. Glass was modified by formation of self assembled monolayers of alkyl siloxanes covalently bonded to the silanol groups on the glass channel walls which led to a variety of further modifications to achieve tunable surface chemistry. However, the fabrication of glass microchips is often expensive, time consuming and the process involves the use of harmful chemicals. These disadvantages have led us to seek alternative solutions for fabricating glass-based microchips.

In chapter 4, a novel and effective means of producing PTFE/glass microfluidic devices was successfully described. The channel was formed by cutting a PTFE sheet using a cutting plotter. The hybrid glass-PTFE microfluidic device was

fabricated using a chemically activated PTFE sheet as a spacer between two chemically activated glass substrates. The glass surface, with amine terminal groups, was bonded to a PTFE sheet surface via an EDC-NHS coupling agent.

In conclusion, the integration of microfluidic devices and spiropyran dyes to yield a photoactivable extraction system for metal ion accumulation and release was realized. Spiropyrans have shown great potential as stimuli-responsive materials, a rapidly expanding area allowing a range of new materials to be prepared for diverse applications. The structural changes in the spiropyran moiety also regulate other properties of the material, for example, viscosity, solubility, and its refractive index [1, 2]; this inspiring control over bulk material properties creates numerous opportunities for the design of "smart" materials where properties can be regulated through controlled input.

5.1. References

1.   Irie, M., A. Menju, and K. Hayashi, *Photoresponsive Polymers. Reversible Solution Viscosity Change of Poly(methyl methacrylate) Having Spirobenzopyran Side Groups.* Macromolecules, 1979. **12**(6): p. 1176-1180.

2.   Konak, C., et al., *Photoregulated Association of Water-Soluble Copolymers with Spirobenzopyran-Containing Side Chains.* Macromolecules, 1997. **30**(18): p. 5553-5556.

BIBLIOGRAPHY

1.   Crano, J.C. and R.J. Guglielmetti, *Organic photochromic and thermochromic compounds*. Topics in applied chemistry. 1999, New York: Kluwer Academic/Plenum Publishers.

2.   Ercole, F., T.P. Davis, and R.A. Evans, *Photo-responsive systems and biomaterials: photochromic polymers, light-triggered self-assembly, surface modification, fluorescence modulation and beyond.* Polymer Chemistry, 2010. **1**(1): p. 37-54.

3.   Kato, N., et al., *In Situ Observation of the Thermochromic Phase Transition of the Merocyanine J-Aggregates Monolayer at the Air-Water Interface Using External Infrared Reflection Absorption Spectroscopy.* The Journal of Physical Chemistry B, 2003. **107**(43): p. 11917-11923.

4.   Mishra, A., et al., *Cyanines during the 1990s: A Review.* Chemical Reviews, 2000. **100**(6): p. 1973-2012.

5.   Kimura, K., et al., *Cation complexation, photochromism, and aggregation of copolymers carrying crown ether and spirobenzopyran moieties at the side chains.* Bulletin of the Chemical Society of Japan, 2003. **76**(1): p. 209-215.

6.   Nakatsuji, S., et al., *Novel photo-responsive organic spin systems: preparation and properties of norbornadienes and spiropyrans with TEMPO radical*

substituents. Journal of the Chemical Society-Perkin Transactions 2, 2000(9): p. 1969-1975.

7.   Benniston, A.C., et al., *Opening a spiropyran ring by way of an exciplex intermediate.* Journal of Organic Chemistry, 2007. **72**(3): p. 888-897.

8.   Botrel, A., et al., *A theoretical investigation of solvatochromism. Application to merocyanines similar to colored forms obtained by flash-photolysis of spiropyrans.* Chemical Physics, 1995. **194**(1): p. 101-116.

9.   Matsumoto, M., et al., *Light-induced J-aggregation of merocyanine in Langmuir and Langmuir-Blodgett films.* Journal of Physical Chemistry B, 2002. **106**(44): p. 11487-11491.

10.   Delaire, J.A. and K. Nakatani, *Linear and Nonlinear Optical Properties of Photochromic Molecules and Materials.* Chemical Reviews, 2000. **100**(5): p. 1817-1846.

11.   Berkovic, G., V. Krongauz, and V. Weiss, *Spiropyrans and Spirooxazines for Memories and Switches.* Chemical Reviews, 2000. **100**(5): p. 1741-1754.

12.   Abe, S., et al., *Remarkable electric field effect on the absorption intensity of a molecular aggregate of photomerocyanine in a PMMA polymer film.* Chemistry Letters, 1999(2): p. 165-166.

13.   Plaza, P., et al., *Reversible bulk photorelease of strontium ion from a crown ether-linked merocyanine.* Chemphyschem, 2002. **3**(8): p. 668-674.

14.   Onai, Y., et al., *COLORED MEROCYANINE AGGREGATES - LONG-LIVED CRYSTALS OF LARGE-SIZE (10-100-MU-M) AND DEAGGREGATION OF SMALL AGGREGATES IN SOLUTIONS.* Journal of Physical Chemistry, 1993. **97**(37): p. 9499-9505.

15.   Garcia, A., et al., *Photo-, thermally, and pH-responsive microgels.* Langmuir, 2007. **23**(1): p. 224-229.

16.   Winkler, J.D., C.M. Bowen, and V. Michelet, *Photodynamic Fluorescent Metal Ion Sensors with Parts per Billion Sensitivity.* Journal of the American Chemical Society, 1998. **120**(13): p. 3237-3242.

17.   Benniston, A.C. and J. Fortage, *Selenospiropyrans incorporating appended pyrene chromophores.* Tetrahedron Letters, 2008. **49**(27): p. 4292-4295.

18.   Kinashi, K., Y. Harada, and Y. Ueda, *Thermal stability of merocyanine form in spiropyran/silica composite film.* Thin Solid Films, 2008. **516**(9): p. 2532-2536.

19.   Benard, S., et al., *Interplay between magnetism and photochromism in spiropyran-MnPS3 intercalation compounds.* Chemistry of Materials, 2001. **13**(10): p. 3709-3716.

20.   Bouas-Laurent, H. and H. Dürr, *Organic photochromism (IUPAC Technical Report).* Pure and Applied Chemistry, 2001. **73**(4): p. 639-665.

21. Di Benedetto, F., et al., *Photoswitchable organic nanofibers.* Advanced Materials, 2008. **20**(2): p. 314-318.

22. Fries, K., et al., *Reversible colorimetric ion sensors based on surface initiated polymerization of photochromic polymers.* Chemical Communications, 2008(47): p. 6288-6290.

23. Roxburgh, C.J., P.G. Sammes, and A. Abdullah, *Photoreversible Zn2+ Ion Transportation Across an Interface Using Ion-Chelating Substituted Photochromic 3,3 '-Indolospirobenzopyrans: Steric and Electronic Controlling Effects.* European Journal of Inorganic Chemistry, 2008(31): p. 4951-4960.

24. Shao, N., et al., *Spiropyran-based fluorescent probes for biological species.* Luminescence, 2008. **23**(2): p. 91-91.

25. George, M.C., et al., *Direct Laser Writing of Photoresponsive Colloids for Microscale Patterning of 3D Porous Structures.* Advanced Materials, 2009. **21**(1): p. 66-70.

26. Yagi, S., et al., *Colorimetric sensing of metal ions by bis(spiropyran) podands: Towards naked-eye detection of alkaline earth metal ions.* Dyes and Pigments, 2009. **80**(1): p. 98-105.

27. Heiligman-Rim, R., Y. Hirshberg, and E. Fischer, *PHOTOCHROMISM IN SPIROPYRANS. PART V.1 ON THE MECHANISM OF*

PHOTOTRANSFORMATION. The Journal of Physical Chemistry, 1962. **66**(12): p. 2470-2477.

28.   Gorner, H., *Photoprocesses in spiropyrans and their merocyanine isomers: Effects of temperature and viscosity.* Chemical Physics, 1997. **222**(2-3): p. 315-329.

29.   Chibisov, A.K. and H. Gorner, *Photoprocesses in spiropyran-derived merocyanines.* Journal of Physical Chemistry A, 1997. **101**(24): p. 4305-4312.

30.   Yagi, S., K. Maeda, and H. Nakazumi, *Photochromic properties of cationic merocyanine dyes. Thermal stability of the spiropyran form produced by irradiation with visible light.* Journal of Materials Chemistry, 1999. **9**(12): p. 2991-2997.

31.   Chibisov, A.K. and H. Gorner, *Singlet versus triplet photoproceses in indodicarbocyanine dyes and spiropyran-derived merocyanines.* Journal of Photochemistry and Photobiology a-Chemistry, 1997. **105**(2-3): p. 261-267.

32.   Gorner, H., *Photochemical ring opening in nitrospiropyrans: triplet pathway and the role of singlet molecular oxygen.* Chemical Physics Letters, 1998. **282**(5-6): p. 381-390.

33.   Haupl, T., et al., *The Competitive Effect of Intramolecular Charge Transfer on the Photochromism of Spiro[cyclohexadiene-indolines] Studied by ps-*

Spectroscopy. The Journal of Physical Chemistry A, 1999. **103**(35): p. 6904-6910.

34. Hobley, J., et al., *Proton exchange and isomerisation reactions of photochromic and reverse photochromic spiro-pyrans and their merocyanine forms.* Physical Chemistry Chemical Physics, 1999. **1**(14): p. 3259-3267.

35. Bouas-Laurent, H., et al., *Organic Photochromism*, in *Photochromism.* 2003, Elsevier Science: Amsterdam. p. XXVII-LIII.

36. Tanaka, M., et al., *Synthesis and photochromism of spirobenzopyran derivatives bearing an oxymethylcrown ether moiety: Metal ion-induced switching between positive and negative photochromisms.* Journal of Organic Chemistry, 2001. **66**(5): p. 1533-1537.

37. Byrne, R. and D. Diamond, *Chemo/bio-sensor networks.* Nature Materials, 2006. **5**(6): p. 421-424.

38. Crano, J.C., et al., *Photochromic compounds: Chemistry and application in ophthalmic lenses.* Pure and Applied Chemistry, 1996. **68**(7): p. 1395-1398.

39. Raymo, F.M. and S. Giordani, *All-optical processing with molecular switches.* Proceedings of the National Academy of Sciences of the United States of America, 2002. **99**(8): p. 4941-4944.

40. Radu, A., et al., *Photonic modulation of surface properties: a novel concept in chemical sensing.* Journal of Physics D-Applied Physics, 2007. **40**(23): p. 7238-7244.

41. Kelly, J.M., C.B. McArdle, and M.J.d.F. Maunder, *Photochemistry and Polymeric Systems*. Photochromic organic compounds in polymer matrices, ed. J.C. Crano, et al. 1993, Cambridge: Royal Society of Chemistry. 179-193.

42. Bertelson, R.C., *REMINISCENCES ABOUT ORGANIC PHOTOCHROMICS.* Molecular Crystals and Liquid Crystals Science and Technology Section a-Molecular Crystals and Liquid Crystals, 1994. **246**: p. 1-8.

43. Evans, L., et al., *Selective Metals Determination with a Photoreversible Spirobenzopyran.* Analytical Chemistry, 1999. **71**(23): p. 5322-5327.

44. Collins, G.E., et al., *Photoinduced switching of metal complexation by quinolinospiropyranindolines in polar solvents.* Chemical Communications, 1999(4): p. 321-322.

45. Leaustic, A., et al., *Photochromism of cationic spiropyran-doped silica gels.* New Journal of Chemistry, 2001. **25**(10): p. 1297-1301.

46. Shao, N., et al., *Copper ion-selective fluorescent sensor based on the inner filter effect using a spiropyran derivative.* Analytical Chemistry, 2005. **77**(22): p. 7294-7303.

47.   Inouye, M., et al., *Alkali metal recognition induced isomerization of spiropyrans.* Journal of the American Chemical Society, 1990. **112**(24): p. 8977-8979.

48.   Tian, Z.Y., et al., *Single-Chromophore-Based Photoswitchable Nanoparticles Enable Dual-Alternating-Color Fluorescence for Unambiguous Live Cell Imaging.* Journal of the American Chemical Society, 2009. **131**(12): p. 4245-4252.

49.   Kinashi, K., et al., *Multi-photochromic behavior of hybrid material with spirobenzopyran and azobenzene moieties.* Chemistry Letters, 2006. **35**(3): p. 298-299.

50.   Kimura, K., T. Teranishi, and M. Yokoyama, *Highly calcium-ion-accelerated coloration of bis(spirobenzopyran) bridged by diaza-18-crown-6 moiety at the 8-position.* Supramolecular Chemistry, 1996. **7**(1): p. 11-13.

51.   Kimura, K., H. Sakamoto, and T. Nakamura, *Application of photoresponsive polymers carrying crown ether and spirobenzopyran side chains to photochemical valve.* Journal of Nanoscience and Nanotechnology, 2006. **6**(6): p. 1741-1749.

52.   Kimura, K., M. Sumida, and M. Yokoyama, *Drastic metal-ion enhancement in photoinduced aggregation of copolymers carrying crown ether and*

spirobenzopyran moieties. Chemical Communications, 1997(15): p. 1417-1418.

53. Shao, N., et al., *Design of Bis-spiropyran Ligands as Dipolar Molecule Receptors and Application to in Vivo Glutathione Fluorescent Probes.* Journal of the American Chemical Society, 2010. **132**(2): p. 725-736.

54. Tomizaki, K.Y., X. He, and H. Mihara, *A chromism-based assay (CHROBA) technique for in situ detection of protein kinase activity.* Bioorganic & Medicinal Chemistry Letters, 2005. **15**(6): p. 1731-1735.

55. Tomizaki, K. and H. Mihara, *PHOTOCHROMIC SPIROPYRAN-CONTAINING PEPTIDES FOR A NOVEL PROTEIN DETECTING SYSTEM.* Journal of Peptide Science, 2004. **10**: p. 158-158.

56. Manz, A., et al., *Micromachining of monocrystalline silicon and glass for chemical analysis systems A look into next century's technology or just a fashionable craze?* TrAC Trends in Analytical Chemistry, 1991. **10**(5): p. 144-149.

57. Jacobson, S.C., et al., *Effects of Injection Schemes and Column Geometry on the Performance of Microchip Electrophoresis Devices.* Analytical Chemistry, 1994. **66**(7): p. 1107-1113.

58.   Harrison, D.J., et al., *Capillary electrophoresis and sample injection systems integrated on a planar glass chip.* Analytical Chemistry, 1992. **64**(17): p. 1926-1932.

59.   Kikutani, Y., et al., *Glass microchip with three-dimensional microchannel network for 2 [times] 2 parallel synthesis.* Lab on a Chip, 2002. **2**(4): p. 188-192.

60.   Kikutani, Y., et al., *Pile-up glass microreactor.* Lab on a Chip, 2002. **2**(4): p. 193-196.

61.   Wang, H.Y., et al., *Low temperature bonding for microfabrication of chemical analysis devices.* Sensors and Actuators B: Chemical, 1997. **45**(3): p. 199-207.

62.   Akiyama, Y., et al., *Rapid bonding of Pyrex glass microchips.* Electrophoresis, 2007. **28**(6): p. 994-1001.

63.   Wallis, G., *DIRECT-CURRENT POLARIZATION DURING FIELD-ASSISTED GLASS-METAL SEALING.* Journal of the American Ceramic Society, 1970. **53**(10): p. 563-&.

64.   Sayah, A., et al., *Development of novel low temperature bonding technologies for microchip chemical analysis applications.* Sensors and Actuators A: Physical, 2000. **84**(1-2): p. 103-108.

65.   Chiem, N., et al., *Room temperature bonding of micromachined glass devices for capillary electrophoresis.* Sensors and Actuators B: Chemical, 2000. **63**(3): p. 147-152.

66.   Xia, Y.N. and G.M. Whitesides, *Soft lithography.* Angewandte Chemie-International Edition, 1998. **37**(5): p. 551-575.

67.   Xia, Y.N. and G.M. Whitesides, *Soft lithography.* Annual Review of Materials Science, 1998. **28**: p. 153-184.

68.   Jeon, N.L., et al., *Fabrication of silicon MOSFETs using soft lithography.* Advanced Materials, 1998. **10**(17): p. 1466-1469.

69.   Tsao, C.W. and D.L. DeVoe, *Bonding of thermoplastic polymer microfluidics.* Microfluidics and Nanofluidics, 2009. **6**(1): p. 1-16.

70.   Martynova, L., et al., *Fabrication of plastic microfluid channels by imprinting methods.* Analytical Chemistry, 1997. **69**(23): p. 4783-4789.

71.   Xu, J.D., et al., *Room-temperature imprinting method for plastic microchannel fabrication.* Analytical Chemistry, 2000. **72**(8): p. 1930-1933.

72.   McCormick, R.M., et al., *Microchannel electrophoretic separations of DNA in injection-molded plastic substrates.* Analytical Chemistry, 1997. **69**(14): p. 2626-2630.

73.   Giselbrecht, S., et al., *3D tissue culture substrates produced by microthermoforming of pre-processed polymer films.* Biomedical Microdevices, 2006. **8**(3): p. 191-199.

74.   Yuan, D.J. and S. Das, *Experimental and theoretical analysis of direct-write laser micromachining of polymethyl methacrylate by CO_2 laser ablation.* Journal of Applied Physics, 2007. **101**(2).

75.   Cheng, J.-Y., et al., *Direct-write laser micromachining and universal surface modification of PMMA for device development.* Sensors and Actuators B: Chemical, 2004. **99**(1): p. 186-196.

76.   Brister, P.C. and K.D. Weston, *Patterned Solvent Delivery and Etching for the Fabrication of Plastic Microfluidic Devices.* Analytical Chemistry, 2005. **77**(22): p. 7478-7482.

77.   Becker, H. and C. Gärtner, *Polymer microfabrication technologies for microfluidic systems.* Analytical and Bioanalytical Chemistry, 2008. **390**(1): p. 89-111.

78.   Chen, Q., et al., *Light-Triggered Self-Assembly of a Spiropyran-Functionalized Dendron into Nano-/Micrometer-Sized Particles and Photoresponsive Organogel with Switchable Fluorescence.* Advanced Functional Materials. **20**(1): p. 36-42.

79.   Galloway, M., et al., *Contact Conductivity Detection in Poly(methyl methacylate)-Based Microfluidic Devices for Analysis of Mono- and Polyanionic Molecules.* Analytical Chemistry, 2002. **74**(10): p. 2407-2415.

80.   Chen, Z., et al., *Vacuum-assisted thermal bonding of plastic capillary electrophoresis microchip imprinted with stainless steel template.* Journal of Chromatography A, 2004. **1038**(1-2): p. 239-245.

81.   Kelly, R.T. and A.T. Woolley, *Thermal Bonding of Polymeric Capillary Electrophoresis Microdevices in Water.* Analytical Chemistry, 2003. **75**(8): p. 1941-1945.

82.   Klank, H., J.P. Kutter, and O. Geschke, *CO_2-laser micromachining and back-end processing for rapid production of PMMA-based microfluidic systems.* Lab on a Chip, 2002. **2**(4): p. 242-246.

83.   Yussuf, A.A., et al., *Sealing of polymeric-microfluidic devices by using high frequency electromagnetic field and screen printing technique.* Journal of Materials Processing Technology, 2007. **189**(1-3): p. 401-408.

84.   Tennico, Y.H., et al., *Surface modification-assisted bonding of polymer-based microfluidic devices.* Sensors and Actuators B-Chemical, 2010. **143**(2): p. 799-804.

85.   Rahbar, M., et al., *Microwave-induced, thermally assisted solvent bonding for low-cost PMMA microfluidic devices.* Journal of Micromechanics and Microengineering, 2010. **20**(1).

86.   Koesdjojo, M.T., C.R. Koch, and V.T. Remcho, *Technique for Microfabrication of Polymeric-Based Microchips from an SU-8 Master with Temperature-Assisted Vaporized Organic Solvent Bonding.* Analytical Chemistry, 2009. **81**(4): p. 1652-1659.

87.   Kelly, R.T., T. Pan, and A.T. Woolley, *Phase-changing sacrificial materials for solvent bonding of high-performance polymeric capillary electrophoresis microchips.* Analytical Chemistry, 2005. **77**(11): p. 3536-3541.

88.   Griebel, A., et al., *Integrated polymer chip for two-dimensional capillary gel electrophoresis.* Lab on a Chip, 2004. **4**(1): p. 18-23.

89.   Lei, K.F., et al., *Microwave bonding of polymer-based substrates for potential encapsulated micro/nanofluidic device fabrication.* Sensors and Actuators A: Physical, 2004. **114**(2-3): p. 340-346.

90.   Barker, S.L.R., et al., *Plastic Microfluidic Devices Modified with Polyelectrolyte Multilayers.* Analytical Chemistry, 2000. **72**(20): p. 4899-4903.

91.   Cabrera, I., V. Krongauz, and H. Ringsdorf, *PHOTOCHROMIC AND THERMOCHROMIC LIQUID-CRYSTAL POLYMERS WITH SPIROPYRAN GROUPS.* Molecular Crystals and Liquid Crystals, 1988. **155**: p. 221-230.

92.   Unuma, Y. and A. Miyata, *LIGHT-INDUCED MOLECULAR-ORIENTATION IN LANGMUIR-BLODGETT-FILMS OF SPIROPYRAN.* Sharp Technical Journal, 1989(43): p. 45-50.

93.   Pigois, E., et al., *X-RAY PHOTOELECTRON-SPECTROSCOPY OF SPIROPYRAN MOLECULES.* Journal of Electron Spectroscopy and Related Phenomena, 1990. **53**(1-2): p. 79-86.

94.   Kuhn, D., H. Balli, and U.E. Steiner, *KINETIC-STUDY OF THE PHOTODECOLORATION MECHANISM OF AN INVERSELY PHOTOCHROMIC CLASS OF COMPOUNDS FORMING SPIROPYRAN ANALOGS.* Journal of Photochemistry and Photobiology a-Chemistry, 1991. **61**(1): p. 99-112.

95.   Rappon, M., et al., *PHOTOINDUCED REACTION OF DYE IN POLYMER MEDIA .1. UNANNEALED POLYMER MATRICES.* European Polymer Journal, 1991. **27**(4-5): p. 365-370.

96.   Garcia, A.A., et al., *Photon-controlled phase partitioning of spiropyrans.* Journal of Physical Chemistry A, 2000. **104**(26): p. 6103-6107.

97.   Winkler, J.D., K. Deshayes, and B. Shao, *Photodynamic transport of metal ions.* Journal of the American Chemical Society, 1989. **111**(2): p. 769-770.

98. Brown, L., et al., *Fabrication and characterization of poly(methylmethacrylate) microfluidic devices bonded using surface modifications and solvents.* Lab on a Chip, 2006. **6**(1): p. 66-73.

99. Byrne, R.J., S.E. Stitzel, and D. Diamond, *Photo-regenerable surface with potential for optical sensing.* Journal of Materials Chemistry, 2006. **16**(14): p. 1332-1337.

100. Stitzel, S., R. Byrne, and D. Diamond, *LED switching of spiropyran-doped polymer films.* Journal of Materials Science, 2006. **41**(18): p. 5841-5844.

101. Bletz, M., et al., *Ground- and first-excited-singlet-state electric dipole moments of some photochromic spirobenzopyrans in their spiropyran and merocyanine form.* Journal of Physical Chemistry A, 2002. **106**(10): p. 2232-2236.

102. Bakker, E. and Y. Qin, *Electrochemical Sensors.* Analytical Chemistry, 2006. **78**(12): p. 3965-3984.

103. Boone, T., et al., *Plastic advances microfluidic devices.* Analytical Chemistry, 2002. **74**(3): p. 78A-86A.

104. Sun, Y., Y.C. Kwok, and N.T. Nguyen, *Low-pressure, high-temperature thermal bonding of polymeric microfluidic devices and their applications for electrophoretic separation.* Journal of Micromechanics and Microengineering, 2006. **16**(8): p. 1681-1688.

105. Rossier, J., F. Reymond, and P.E. Michel, *Polymer microfluidic chips for electrochemical and biochemical analyses.* Electrophoresis, 2002. **23**(6): p. 858-867.

106. Blanco, F.J., et al., *Novel three-dimensional embedded SU-8 microchannels fabricated using a low temperature full wafer adhesive bonding.* Journal of Micromechanics and Microengineering, 2004. **14**(7): p. 1047-1056.

107. Duffy, D.C., et al., *Rapid prototyping of microfluidic systems in poly(dimethylsiloxane).* Analytical Chemistry, 1998. **70**(23): p. 4974-4984.

108. Tennico, Y.H., et al., *Surface modification-assisted bonding of polymer-based microfluidic devices.* Sensors and Actuators B: Chemical, 2010. **143**(2): p. 799-804.

109. Koesdjojo, M.T., Y.H. Tennico, and V.T. Reincho, *Fabrication of a microfluidic system for capillary electrophoresis using a two-stage embossing technique and solvent welding on poly(methyl methacrylate) with water as a sacrificial layer.* Analytical Chemistry, 2008. **80**(7): p. 2311-2318.

110. Tsao, C.W., et al., *Low temperature bonding of PMMA and COC microfluidic substrates using UV/ozone surface treatment.* Lab on a Chip, 2007. **7**(4): p. 499-505.

111. Vlachopoulou, M.E. and et al., *A low temperature surface modification assisted method for bonding plastic substrates.* Journal of Micromechanics and Microengineering, 2009. **19**(1): p. 015007.

112. Bart, J., et al., *Room-temperature intermediate layer bonding for microfluidic devices.* Lab on a Chip, 2009. **9**(24): p. 3481-3488.

113. Balachander, N. and C.N. Sukenik, *Monolayer transformation by nucleophilic substitution: Applications to the creation of new monolayer assemblies.* Langmuir, 1990. **6**(11): p. 1621-1627.

114. Lee, T.R., et al., *The Wetting of Monolayer Films Exposing Ionizable Acids and Bases.* Langmuir, 1994. **10**(3): p. 741-749.

115. Irie, M., A. Menju, and K. Hayashi, *Photoresponsive Polymers. Reversible Solution Viscosity Change of Poly(methyl methacrylate) Having Spirobenzopyran Side Groups.* Macromolecules, 1979. **12**(6): p. 1176-1180.

116. Konak, C., et al., *Photoregulated Association of Water-Soluble Copolymers with Spirobenzopyran-Containing Side Chains.* Macromolecules, 1997. **30**(18): p. 5553-5556.